Automatic characterization of affective states in individuals with mood disorders based on the analysis of brain-heart interactions

by

Mohammad Hasan AZAD

THESIS PRESENTED TO ÉCOLE DE TECHNOLOGIE SUPÉRIEURE
IN PARTIAL FULFILLMENT OF A MASTER'S DEGREE
WITH THESIS IN ELECTRICAL ENGINEERING
M.A.Sc.

MONTREAL, JUNE 18, 2025

ÉCOLE DE TECHNOLOGIE SUPÉRIEURE
UNIVERSITÉ DU QUÉBEC

BOARD OF EXAMINERS

THIS THESIS HAS BEEN EVALUATED

BY THE FOLLOWING BOARD OF EXAMINERS

Prof. Mohamad Forouzanfar, Thesis supervisor
Department of System Engineering, Ecole de technologie Supérieure, Montreal, Canada

Prof. Rebecca Robillard, Thesis Co-Supervisor
School of Psychology, University of Ottawa, Ottawa, Canada

Prof. Jean-Marc Lina, Thesis Co-Supervisor
Department of Electrical Engineering, Ecole de technologie Supérieure, Montreal, Canada

Prof. Ismail Ben Ayed, Chair, Board of Examiners
Department of System Engineering, Ecole de technologie Supérieure, Montreal, Canada

Prof. Sylvie Ratté, External Examiner
Department of Software and IT Engineering, Ecole de technologie Supérieure, Montreal, Canada

THIS THESIS WAS PRESENTED AND DEFENDED

IN THE PRESENCE OF A BOARD OF EXAMINERS AND THE PUBLIC

ON APRIL 9, 2025

AT ÉCOLE DE TECHNOLOGIE SUPÉRIEURE

ACKNOWLEDGEMENTS

I want to take a moment to express my deepest gratitude to the incredible people who have been part of this chapter of my life. First and foremost, I am truly grateful to my great supervisors, Mohamad, Rebecca, and Jean-Marc, for their invaluable guidance and support throughout my master's. I have learned so much from each of them at every step of this journey.

Beyond academia, my heartfelt thanks go to my family, whom I missed the most during these two and a half years. Not being there for you in difficult times and missing out on our moments together has been the hardest part of this journey. I owe everything to my parents, whose unwavering love and support have been the foundation of all I have achieved. I also deeply missed the fun, the fights, and the companionship of my brothers, Ehsan, Amin, and Amir, who have always been there for me in ways both big and small. A special thanks to my uncle's family—Reza, Banafsheh, Elyda, and Luca—for their incredible support, especially during the first stressful months of immigration.

This journey was also made unforgettable by the amazing friends I met along the way. To my friends in LIVIA and beyond, thank you for the laughs, deep conversations, shared struggles, outdoor adventures, Mafia games, and countless memories that I will carry with me forever. A special shoutout to Gustavo, Julien, Boshra, Fereshteh, Melike, Nima, Milad, Amin, Aryan, Saypraseuth, Masih&Armita, Sina&Parishad, Shivi&Shalesh, Osamah, Haseeb, Heitor, Farzad, Yasaman, Philippe, Maxime, Liam, Paul, Mustapha, Abdoulaye, and many more whose names I may have forgotten—but never the moments we shared. You all made this chapter of my life richer, and I couldn't have asked for better people to share it with.

And finally, to my beloved Reihaneh—no words can fully express how much your presence has meant to me. You have changed my life and filled it with happiness. Through all the challenges and hard times, your support, patience, love, and laughter have been my greatest superpower. Thank you for always being there.

To all of you.

Caractérisation automatique des états affectifs chez les individus atteints de troubles de l'humeur basée sur l'analyse des interactions cerveau-cœur

Mohammad Hasan AZAD

RÉSUMÉ

En 2019, environ 9% de la population canadienne a souffert de troubles de l'humeur, tels que la dépression ou le trouble bipolaire. Le diagnostic et le traitement de ces affections sont souvent freinés par des facteurs comme la stigmatisation sociale, des ressources cliniques limitées, et l'absence de marqueurs objectifs fiables. Pour combler cette lacune, cette thèse explore le potentiel d'intégration de plusieurs bio-signaux qui capturent à la fois l'activité cérébrale et cardiaque, afin de fournir une compréhension plus complète des troubles de l'humeur, en particulier la dépression, pendant le sommeil.

L'objectif de cette recherche est d'examiner les mécanismes pathophysiologiques sous-jacents aux troubles de l'humeur en analysant l'interaction entre les signaux d'électroencéphalogramme (EEG) et d'électrocardiogramme (ECG) pendant le sommeil. Cette étude introduit une mesure de cohérence comme biomarqueur potentiel interrelié pour la dépression, reliant l'activité cérébrale et cardiaque. Une analyse secondaire des données de polysomnographie de 46 personnes souffrant de dépression et de 40 témoins sains a été menée, révélant des différences significatives dans la cohérence cerveau-cœur entre les groupes dépressifs et sains à travers les stades du sommeil et les canaux EEG, en particulier dans les bandes de fréquence de 0 à 8 Hz.

En parallèle, cette thèse développe SleepDepNet, un modèle d'apprentissage profond conçu pour automatiser la détection de la dépression en exploitant des biomarqueurs EEG et ECG, tels que le rapport de puissance relative, la fréquence cardiaque, et la mesure de cohérence introduite. SleepDepNet combine des réseaux de neurones convolutifs avec des réseaux de mémoire à long terme pour analyser les caractéristiques temporelles et spectrales de ces signaux. Le modèle a démontré une haute précision de 98,33% dans la classification de la dépression, validant ainsi l'efficacité de l'utilisation des interactions cerveau-cœur comme outils diagnostiques. Ces résultats suggèrent que l'intégration de l'EEG et de l'ECG, associée aux algorithmes d'apprentissage profond, offre une approche prometteuse pour l'identification objective des troubles de l'humeur et jette les bases de recherches futures sur leur détection et prédiction automatisées.

Mots-clés: dépression, électroencéphalogramme, électrocardiogramme, mesure de cohérence, apprentissage profond, réseaux de neurones convolutifs, mémoire à long terme et court terme, polysomnographie, détection automatisée, diagnostic de la santé mentale

Automatic characterization of affective states in individuals with mood disorders based on the analysis of brain-heart interactions

Mohammad Hasan AZAD

ABSTRACT

In 2019, approximately 9% of the Canadian population experienced mood disorders such as depression or bipolar disorder. The diagnosis and treatment of these conditions are often hindered by factors like social stigma, limited clinical resources, and the lack of reliable objective markers. To address this gap, this thesis explores the potential of integrating multiple bio-signals that capture both brain and heart activity to provide a more comprehensive understanding of mood disorders, particularly depression, during sleep.

The primary aim of this research is to investigate the pathophysiological mechanisms underlying mood disorders by analyzing the interaction between sleep electroencephalogram (EEG) and electrocardiogram (ECG) signals. This study introduces a coherence metric as a potential interrelated biomarker for depression, linking brain and heart activity. A secondary analysis of polysomnography data from 46 individuals with depression and 40 healthy controls was conducted, revealing significant differences in brain-heart coherence of depression and healthy groups across sleep stages and EEG channels, particularly in the 0-8 Hz frequency bands.

In parallel, this thesis develops SleepDepNet, a deep learning model designed to automate the detection of depression by leveraging EEG and ECG biomarkers such as relative power ratio, heart rate, and the introduced coherence metric. SleepDepNet combines convolutional neural networks with long short-term memory networks to analyze the temporal and spectral characteristics of these signals. The model demonstrated a high accuracy of 98.33% in classifying depression, validating the efficacy of using brain-heart interactions as diagnostic tools. These findings suggest that integrating EEG and ECG along with deep learning algorithms offers a promising approach for the objective identification of mood disorders and lays the groundwork for future research into their automated detection and prediction.

Keywords: depression, electroencephalogram, electrocardiogram, coherence metric, deep learning, convolutional neural networks, long short-term memory, polysomnography, automated detection, mental health diagnosis

TABLE OF CONTENTS

Page

LIST OF TABLES

Page

LIST OF FIGURES

Page

LIST OF ABBREVIATIONS

ML	Machine Learning
DL	Deep Learning
MDD	Major Depression Disorder
EEG	Electroencephalogram
ECG	Electrocardiogram
CPSD	Cross Power Spectral Density
CNNs	Convolutional Neural Networks
RNNs	Recurrent Neural Networks
LSTMs	Long Short-Term Memories
STFT	Short-Time Fourier Transform
PSD	Power Spectral Density
NNs	Neural Networks
ReLU	Rectified Linear Unit
GRUs	Gated Recurrent Units
HR	Heart Rate
BPM	Beats Per Minute
HRV	Heart Rate Variability
HF	High-Frequency
LF	Low Frequency

VLF	Very Low Frequency
NREM	Non-Rapid Eye Movement
MI	Mutual Information
REM	Rapid Eye Movement
SWS	Slow-Wave Sleep
STE	Symbolic Transfer Entropy
WPLI	Weighed Phase Lag Index
SVM	Support Vector Machine
EOG	Electrooculogram
RF	Random Forest
BO-ERTC	Bayesian-Optimized Extremely Randomized Trees Classifier
OSAS	Obstructive Sleep Apnea Syndrome
MLP	Multi-Layer Perception
MCT	Multiple Comparison Tests
ANOVA	Analysis of Variance
ROMHC	Royal Ottawa Mental Health Centre
EMG	Electromyogram
BDI	Beck Depression Inventory
AMC	Average Magnitude Coherence
MCV	Mean of EEG-ECG Coherence Values

RPR	Relative Power Ratio
BSP	Band Spectral Power
1D-CNN	1-Dimensional Convolutional Neural Network
ADAM	Adaptive Moment Estimation
CE	Cross-Entropy Loss

LIST OF SYMBOLS AND UNITS OF MEASUREMENTS

δ	Delta
θ	Theta
α	Alpha
β	Beta

INTRODUCTION

0.1 Motivation

Early detection of depression is critical for preventing severe outcomes and improving treatment efficacy. Identifying depressive symptoms at an early stage can avert the progression to chronic depression or suicidal tendencies, thereby enhancing the quality of life for affected individuals. Timely intervention allows healthcare providers to employ more effective treatment strategies, leading to better overall prognoses and faster recovery rates.

Depression has significant public health implications due to its high prevalence and comorbidity with other health conditions. It is a leading cause of disability worldwide, contributing substantially to the global burden of disease Organization. Moreover, depression often coexists with conditions like cardiovascular disease and other mental disorders, necessitating comprehensive management approaches to address both mental and physical health simultaneously Brandenberger, Ehrhart, Piquard & Simon. Effective detection and treatment can thus help mitigate the widespread impact of depression on public health.

0.2 Limitations of depression detection methods

Depression detection methods, including clinical assessments, self-report questionnaires, and automated detection through technology, each have their own set of limitations. Clinical assessments are often subjective, time-consuming, and dependent on the clinician's interpretation, which can vary. They also face issues of stigma and limited access, especially in underserved areas Zhang *et al.* (a); Pinto & Parente. Self-report questionnaires, while accessible, rely heavily on the patient's honesty and self-awareness, and can be influenced by the patient's current state, making them variable and sometimes unreliable.

Conventional machine learning (ML) methods often fall short when it comes to understanding the intricate and multifaceted nature of human emotions. Depression, in particular, presents a unique challenge for these systems, as its fluid and evolving characteristics are difficult to fully capture, leaving gaps in how well the psychological complexities are represented. However, these methods are rapidly advancing, with significant improvements in data accuracy and prediction techniques with deep learning (DL) methods, offering ample opportunities for further exploration in this field Pinto & Parente.

Most depression detection techniques are typically applied during a patient's resting state, where the individual is not engaged in any cognitive or physical tasks. This ensures that external activities do not interfere with the accuracy of the analysis. Sleep, being an ideal form of resting state where the individual is completely inactive, offers a valuable opportunity for analyzing data in the context of depression detection Zhang *et al.* (a). Studying sleep patterns can provide deeper insights into the disorder, as it allows for the observation of brain and body functions without interference from cognitive or physical activities. Additionally, over 90% of individuals experiencing sleep disturbances are diagnosed with depression, which further emphasizes the relevance of utilizing sleep data for detecting and understanding this disorder Tsuno, Besset, Ritchie *et al.* (2005). This strong association between sleep difficulties and depression makes sleep analysis a valuable tool in the diagnostic process.

These limitations highlight the need for continued research and a combined approach that integrates multiple methods for a more accurate and comprehensive understanding of depression.

0.3 Problem statement

To overcome the limitations of current depression detection methods, we can adopt an engineering perspective. This approach allows us to explore and develop solutions for automated detection methods, aiming to enhance their speed and accuracy. By focusing on technological

advancements, we can improve depression detection more effectively compared to traditional methods.

Analyzing sleep data is a promising way to collect useful information about mental disorders. Since sleep data are recorded while a patient is asleep, they provide unadulterated information about different body systems involved in the recordings Zhang *et al.* (a). Specifically, brain and heart signals recorded during sleep offer critical insights, as these two body systems are primary sources of depression biomarkers Pinto & Parente. We aim to analyze brain and heart signals both separately and in conjunction to better understand and expand existing biomarkers of depression.

To comprehend the relationships between the brain and heart, we need to conduct a comprehensive investigation into the potential interactions between these two critical physiological systems. This exploration aims to determine whether there are any interdependent biomarkers of depression present within the interactions between brain and heart signals. Understanding these relationships is crucial for advancing our knowledge of how depression manifests and can be detected through physiological signals.

Moreover, we intend to employ automated prediction techniques to process the input data and predict whether an individual is experiencing depression. ML and DL techniques present promising solutions for this task; however, they come with their own set of challenges. One of the primary challenges is selecting the most appropriate model and approach for analyzing the specific input data, which consists of long-recorded sleep signals. The variety of available models necessitates a thorough evaluation to identify the best-suited approach for our depression detection task.

This thesis will address two main objectives: First, we plan to develop a method to understand the interactions between the brain and the heart that can aid in detecting depression, which will be

addressed in the second chapter of this thesis. Second, we will implement an automated system that can utilize the comprehensive brain-heart data recorded from a patient during sleep to detect mental disorders, specifically major depression. This issue is presented in the third chapter of this dissertation. By achieving these objectives, we hope to contribute to the development of more accurate and efficient depression detection methods, ultimately improving outcomes for individuals suffering from this debilitating disorder.

0.4 Contributions

In this dissertation, we demonstrate how the proper selection of DL algorithms can lead to the accurate detection of major depressive disorder (MDD). Additionally, we highlight that these approaches are not limited to depression detection alone; they can be applied to other problems with similar characteristics, showcasing their versatility and broad applicability.

This thesis makes two main contributions. First, it introduces a coherence metric that represents the interconnected relationship between the brain and heart. This metric analyzes electroencephalogram (EEG) and electrocardiogram (ECG) signals recorded during sleep from different individuals to identify interactions between these two signals. By analyzing the interaction between EEG and ECG signals in the frequency domain, this metric aims to uncover how the brain and heart influence each other, as reflected in their signal characteristics, to aid in the detection of depression. The results of this section were published and presented at SLEEP 2024, the 38th annual meeting of the Associated Professional Sleep Societies in Houston, Texas. An application of this coherence metric to the detection of insomnia disorder was presented at the 27th Conference of the European Sleep Research Society in Seville, Spain.

Second, this thesis introduces a novel DL approach based on time series analysis, which utilizes the most relevant characteristics of EEG and ECG signals as inputs for depression detection. This approach incorporates the coherence metric discussed earlier as an additional input to a

new network called SleepDepNet. SleepDepNet is a multimodal convolutional neural network specifically designed for depression detection. Its multi-headed design allows it to combine all existing inputs, resulting in a more accurate estimation of depression. As detailed in the following chapters, SleepDepNet outperforms other networks and approaches in the literature, achieving the highest accuracy in depression detection. This network has the potential to be used for clinical purposes in identifying depression in patients in the near future. This work has been submitted to the IEEE Transactions on Biomedical Engineering and is currently under revision.

0.5 Organization

The remainder of this dissertation is structured as follows: Chapter 1 provides essential background information on various definitions pertinent to the thesis. It includes an overview of DL architectures, particularly convolutional neural networks (CNN) and recurrent neural networks (RNN), as well as some important signal processing techniques. Chapter 2 discusses the coherence metric, which reveals the hidden interactions between the brain and heart by analyzing EEG and ECG signals recorded during sleep. Chapter 3 introduces our novel DL model, SleepDepNet, detailing its architecture and comparing its performance in depression detection with other existing models in the literature. Finally, Chapter 4 concludes the dissertation and outlines potential directions for future research.

CHAPTER 1

BACKGROUND

This chapter is divided into two main sections. The first section covers the necessary definitions that need to be understood before progressing to the subsequent chapters. In the second section, we review related work and existing literature relevant to each objective of the dissertation. Initially, we delve into the methods of brain-heart interaction discussed in the literature, examining various studies on this topic. Following that, we explore the research conducted on depression detection with sleep data using ML algorithms. By surveying these existing studies, we gain a comprehensive understanding of the current state of research in our field, enabling us to better compare our work with existing methodologies.

1.1 Necessary definitions

In this section, we outline the essential definitions necessary for understanding the subsequent chapters. First, we provide the background of frequency domain analysis, which is a prerequisite for our coherence metric. We discuss cross power spectral density (CPSD), the foundation of the coherence metric, which analyzes the dependencies between EEG and ECG signals. Additionally, we cover the background on DL algorithms required to comprehend our SleepDepNet architecture. We explain key networks such as convolutional neural networks (CNNs), recurrent neural networks (RNNs), and long short-term memories (LSTMs), which are critical concepts for grasping the fundamentals of our proposed network. Finally, we offer an overview of the physiological signals employed, such as EEG and ECG.

1.1.1 Frequency Domain Analysis

There are various methods and domains for analyzing signals, which can be categorized into three main types: time domain, frequency domain, and time-frequency domain analysis Rangayyan & Krishnan (2024). The time domain is the most intuitive, observing the signal's amplitude changes as they occur over time. In contrast, the frequency domain represents the

signal in terms of its constituent frequencies, typically obtained through mathematical transforms such as the Fourier Transform. The time-frequency domain combines both time and frequency information, making it particularly useful for analyzing non-stationary signals that vary over time. Methods such as the Short-Time Fourier Transform (STFT) and Wavelet Transform are commonly used in this domain. Frequency domain analysis is particularly useful for examining the relationship between signals with different characteristics. Given that we are working with physiological signals such as EEG and ECG, which have an inherent periodic nature, analyzing these in the frequency domain can yield more insightful information. This approach allows us to filter out noise and isolate specific frequencies of interest, thereby enhancing signal clarity and removing artifacts. Additionally, frequency domain methods enable us to focus on distinct frequencies for more detailed analysis. These advantages make frequency domain analysis the primary choice for investigating interactions between EEG and ECG signals.

1.1.1.1 Fourier Transform

The Fourier Transform converts a time-domain signal $x[n]$ into its frequency domain representation $X(f)$:

$$X(f) = \mathcal{F}\{x[n]\} = \sum_{n=0}^{N-1} x[n] e^{-j\frac{2\pi}{N}kn} \tag{1.1}$$

where $x[n]$ is the discrete time domain signal, $X(f)$ is the discrete frequency representation of the signal, N is the number of time samples, n is the discrete time, f represents frequency in Hz, and $\mathcal{F}$ denotes the Fourier Transform Rangayyan & Krishnan (2024).

1.1.1.2 Power Spectral Density and Cross Power Spectral Density

The power spectral density (PSD) represents the power distribution of a signal across different frequencies Rangayyan & Krishnan (2024). It can be used to identify the dominant frequencies in a signal. PSD can be defined as the Fourier transform of the autocorrelation function of a

signal, which came as the following equation for a discrete signal:

$$S_{xx}(f) = \mathcal{F}\{R_{xx}[m]\} = \mathcal{F}\left\{\sum_{n=-\infty}^{\infty} x[n]x^*[n-m]\right\} \tag{1.2}$$

where $S_{xx}(f)$ is the PSD of a discrete signal, $R_{xx}[m]$ is the autocorrelation function of the signal $x[n]$, and $x^*[n-m]$ is the complex conjugate of $x[n-m]$.

On the other hand, the CPSD extends the concept of PSD to analyze the relationship between two signals in the frequency domain Jirsa & Müller (2013). It measures how much power is shared between two signals at each frequency, providing insights into their interaction as shown in Figure 1.1. For two discrete time signals $x[n]$, and $y[n]$, the CPSD $S_{xy}(f)$ is as follows:

$$S_{xy}(f) = \mathcal{F}\{R_{xy}[m]\} = \mathcal{F}\left\{\sum_{n=-\infty}^{\infty} x[n]y^*[n-m]\right\} \tag{1.3}$$

where CPSD is the Fourier transform of the cross-correlation between the two signals x and y. Figure 1.1 shows the analysis of the CPSD for a 30-second epoch of ECG and EEG signals. The top graph depicts the PSD of the ECG signal, while the middle graph highlights the PSD of the EEG signal. The bottom graph demonstrates the CPSD between the ECG and EEG signals.

1.1.2 Machine Learning

ML is a branch of artificial intelligence that emphasizes the creation of algorithms and statistical models, allowing computers to execute tasks autonomously without the need for explicit instructions. By leveraging data-driven approaches, ML algorithms have the capability to learn from data, recognize patterns, and generate predictions or decisions based on new information. The essence of ML lies in its ability to improve performance as more data becomes available, making it particularly valuable in a variety of applications, from finance and healthcare to marketing and robotics.

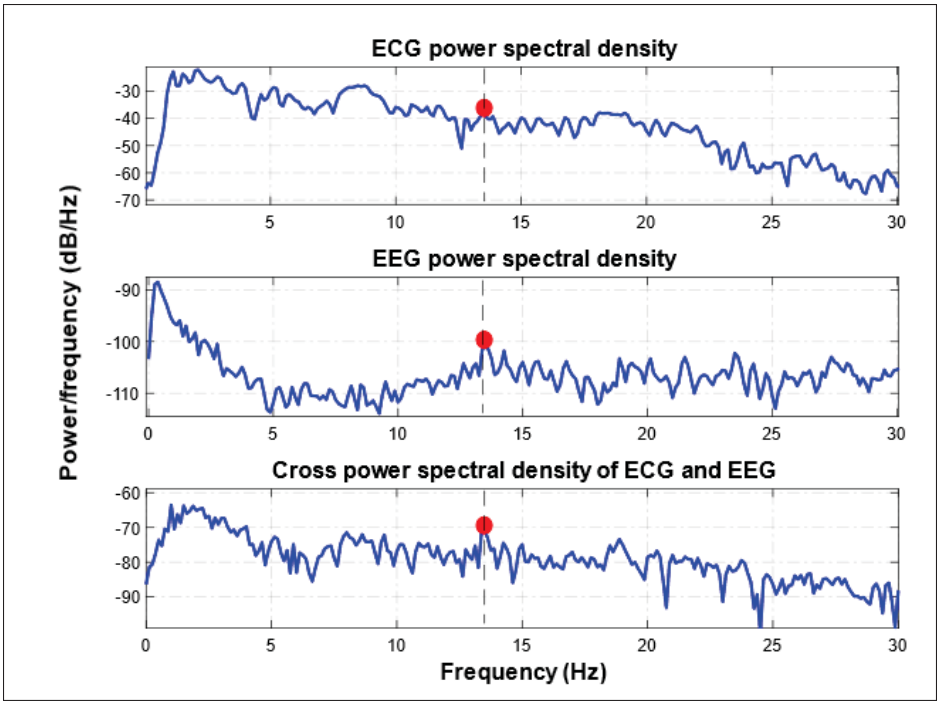

Figure 1.1 CPSD Analysis for a 30-Second Epoch of ECG and EEG Signals. The top plot displays the PSD of ECG, the middle plot shows the PSD of EEG, and the bottom plot illustrates the CPSD between ECG and EEG. All plots are presented in the frequency range of 0 to 30 Hz

In the context of time series analysis, conventional ML algorithms struggle to capture the temporal dependencies inherent in long, continuous signals. In contrast, DL excels at managing and extracting insights from large datasets characterized by complex relationships. When analyzing long recorded signals, such as time series data, DL models can effectively learn from these extensive datasets, uncovering intricate patterns that traditional models might overlook. Unlike conventional ML techniques, which often require manual feature engineering, DL models automatically learn and extract relevant features from raw time series data. This capability is particularly advantageous for long signals, where significant patterns may not be immediately apparent. Additionally, time series data often contain noise or irregularities due to factors like measurement errors or external disturbances. DL models, particularly those employing recurrent architectures, are specifically designed to manage sequential data and effectively filter out this noise, leading to more accurate predictions Goodfellow *et al.* (2016).

1.1.2.1 Deep Learning

To classify depression in sleep signals, which are temporal data, we need to use DL algorithms that account for the time dependency of the input signals. In this section, we explain the key definitions and networks that are prerequisites for understanding our SleepDepNet architecture in the upcoming chapters including CNNs, RNNs, and LSTMs.

1.1.2.2 Convolution Neural Networks (CNNs)

CNNs are a class of DL algorithms designed primarily for processing structured grid two-dimensional data, such as images Goodfellow *et al.* (2016). CNNs have proven highly effective in tasks such as image recognition, object detection, and more recently, in processing sequential and temporal data like time series. This network is composed of some principal components including convolutional layers, activation functions, pooling layers, fully connected layers, and an output layer.

Convolutional layers are the core components of CNNs, and their primary function is to perform convolution operations on the input data using a set of learnable kernels. The size and dimensionality of these kernels can vary depending on the specific task. Kernels can be one-dimensional, two-dimensional, or three-dimensional, corresponding to the nature of the input data Goodfellow *et al.* (2016). In our application, we utilize a one-dimensional kernel that slides over the input data, performing element-wise multiplications and summing the results to produce new feature maps. Each convolutional layer in a CNN is designed to extract increasingly complex features from the data, and a typical CNN architecture consists of multiple such layers. As the data passes through successive layers, the network captures more detailed and abstract representations, enhancing its ability to analyze and classify the input effectively. Mathematically, the convolution operation for a given one-dimensional input X, kernel W, and kernel size m is expressed as the following equation:

$$(X * W)(i, 1) = \sum_{m} X(i - m, 1) W(m, 1) \tag{1.4}$$

By applying this operation, CNN can capture the spatial and temporal information of the data.

To effectively capture the relationship between inputs and outputs through the network layers, we need to introduce nonlinearity. This nonlinearity is provided by the activation function, a crucial component that sets neural networks (NNs) apart from traditional ML algorithms. After passing through each layer, the input is transformed by the activation function, enabling the network to model complex patterns and relationships. The choice of activation function is application-dependent. For our classification task, the Rectified Linear Unit (ReLU) activation function is particularly effective, as it enhances the network's ability to discriminate between different classes. The ReLU function is defined as:

$$\mathrm{ReLU}(x) = \max(0, x) \tag{1.5}$$

Pooling layers reduce the spatial dimensions of the feature maps by aggregating values within each window, making computations more efficient and providing translation invariance Goodfellow *et al.* (2016). This means the network becomes less sensitive to the exact position of features within the input. Common pooling operations include max pooling, average pooling, and global pooling. Max pooling selects the maximum value within each window of the feature map, effectively capturing the most prominent feature in each region and enhancing robustness to variations and noise. The max pooling operation is defined as follows:

$$\mathrm{MaxPooling}(X) = \max_{m \in \mathrm{pool}} X(i + m, 1) \tag{1.6}$$

After several convolutional and pooling layers, the network extracts high-level features that encapsulate the essential information from the input data. These high-level features are then passed to fully connected or dense layers. The fully connected layers combine these extracted features to perform classification or regression tasks. The final fully connected layer produces the output, which in classification tasks discriminates between classes by assigning probabilities.

This is achieved using an appropriate activation function, such as softmax, which is used for both binary and multi-class classification. The softmax function assigns probabilities to each class, indicating the likelihood that the input belongs to each class.

$$\text{softmax}(z_i) = \frac{e^{z_i}}{\sum_j e^{z_j}} \tag{1.7}$$

where z_i represents the score or logit for class i, and the denominator is the sum of the exponentials of the scores for all classes j, ensuring that the probabilities for all classes sum to 1. Figure **??** illustrates LeNet, a well-known CNN architecture, to provide a clear understanding of CNN structural designs.

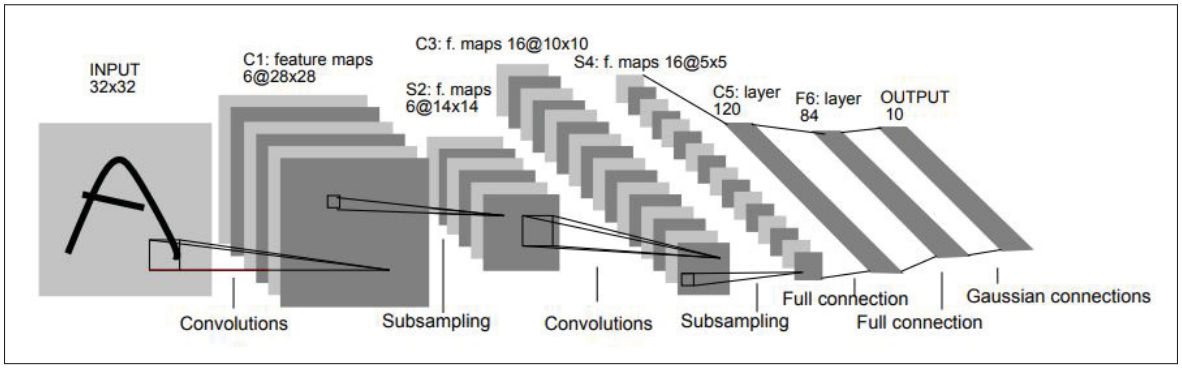

Figure 1.2 LeNET, An example of a famous CNN architecture as illustrated in the original paper
Taken from Lecun *et al.*

1.1.2.3 Recurrent Neural Networks (RNNs)

RNNs are a class of NNs designed to handle sequential data, making them particularly suitable for tasks where the order and context of the data are important, such as time series analysis, natural language processing, and speech recognition Goodfellow *et al.* (2016). RNNs are designed so that somehow connections between nodes can create a cycle, allowing information to persist during the time. Unlike traditional feedforward NNs, RNNs have internal states that act as memory, enabling them to capture temporal dependencies in sequential data. Moreover, RNNs have the

ability to share learned features across different positions in a time series, making predictions more reliable by capturing information throughout the entire sequence. These networks are also capable of handling effectively inputs and outputs of varying lengths, a flexibility that traditional NNs lack. As a result, RNNs are particularly well-suited for applications involving sequential data, where the context and order of information are crucial for accurate predictions.

A basic RNN structure is composed of multiple neurons and layers. In an RNN, each neuron receives input from the previous layer and also transmits information either to itself or to the next time step. In terms of the number of layers, an RNN usually consists of an input layer, one or many recurrent layers, and an output layer Goodfellow *et al.* (2016).

The primary distinguishing feature of RNNs is their ability to maintain a hidden state that captures information from previous time steps. This is achieved through a feedback loop within the network architecture, where the output from the previous time step is fed back into the network along with the current input. Mathematically, the hidden state h_t at time step t can be described by the following equation:

$$h_t = g(W_h \cdot h_{t-1} + W_x \cdot x_t + b_h) \tag{1.8}$$

where h_t and h_{t-1} are the hidden states of the current and previous time steps, respectively. x_t is the input of the network at the time step t. W_h and W_x are the weights matrices. b_h is the bias term and g is a non-linear activation function, which is typically a ReLU or tanh activation function. Figure 1.3 illustrates the general architecture of an one-layer RNN that uses the Eq. 1.8.

While RNNs are powerful, they are also prone to certain challenges, primarily the issues of vanishing and exploding gradients. During backpropagation, gradients can become very small (vanishing gradient problem) or very large (exploding gradient problem), making it difficult for the network to learn long-term dependencies. This is due to the repeated multiplication of

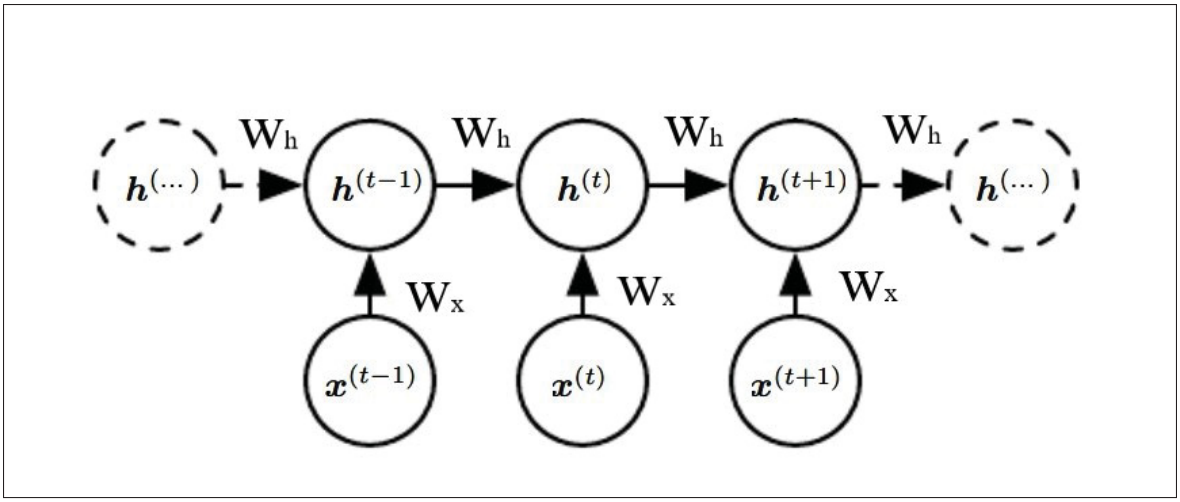

Figure 1.3 An example of an RNN architecture
Taken from Goodfellow *et al.* (2016)

gradients through time steps, which either diminishes the gradient to near zero or amplifies it to infinity.

To address these issues, several variants of RNNs have been developed, most notably LSTMs and Gated Recurrent Units (GRUs), which introduce gating mechanisms to better manage the flow of information and gradients Goodfellow *et al.* (2016).

1.1.2.4 Long-Short-Term Memories (LSTMs)

LSTMs are a specialized form of RNNs designed to overcome the vanishing gradient problem by introducing memory cells that can maintain their state over long periods. Each LSTM cell contains three gates: the input gate, the forget gate, and the output gate Goodfellow *et al.* (2016). These gates regulate the flow of information into, out of, and within the memory cell. The equations governing an LSTM cell at time step t are as follows:

$$f_t = \sigma(W_f \cdot [h_{t-1}, x_t] + b_f) \tag{1.9}$$

$$i_t = \sigma(W_i \cdot [h_{t-1}, x_t] + b_i) \tag{1.10}$$

$$\tilde{C}_t = \tanh(W_C \cdot [h_{t-1}, x_t] + b_C) \tag{1.11}$$

$$C_t = f_t \cdot C_{t-1} + i_t \cdot \tilde{C}_t \tag{1.12}$$

$$o_t = \sigma(W_o \cdot [h_{t-1}, x_t] + b_o) \tag{1.13}$$

$$h_t = o_t \cdot \tanh(C_t) \tag{1.14}$$

where f_t, i_t, and O_t are the forget, input and output's gate activation vector, respectively. $\tilde{C}_t$ is the cell candidate vector, C_t is the cell state vector, and σ is the sigmoid activation function.

The forget gate f_t controls how much of the previous cell state C_{t-1} should be retained, while the input gate i_t determines how much of the new candidate cell state $\tilde{C}_t$ should be added. The output gate O_t decides how much of the cell state should be exposed as the hidden state h_t. This gating mechanism allows LSTMs to maintain long-term dependencies more effectively than traditional RNNs, making them suitable for tasks where understanding long sequences is critical. In the LSTM, cell state C_t plays a key role. This cell is like a longe term memory to help the network deal with the issue of the vanishing gradient. For the input sequence to backpropagate without vanishing gradient problem, it is essential that C_t be highly dependent on C_{t-1}. Figure 1.4 shows the structure of an LSTM cell with its described gates. The input arrows in this figure represent the cell's input, the cell state, and the hidden state.

1.1.3 Physiological Signals: EEG and ECG

1.1.3.1 Electroencephalogram (EEG)

EEG is a non-invasive method used to record electrical activity in the brain. The brain's neurons communicate through electrical impulses, and EEG measures these impulses via electrodes placed on the scalp Rangayyan & Krishnan (2024). EEG is extensively utilized in both clinical and research settings for brain-computer interfacing, monitoring brain activity, assessing sleep stages and brain function, and diagnosing neurological disorders.

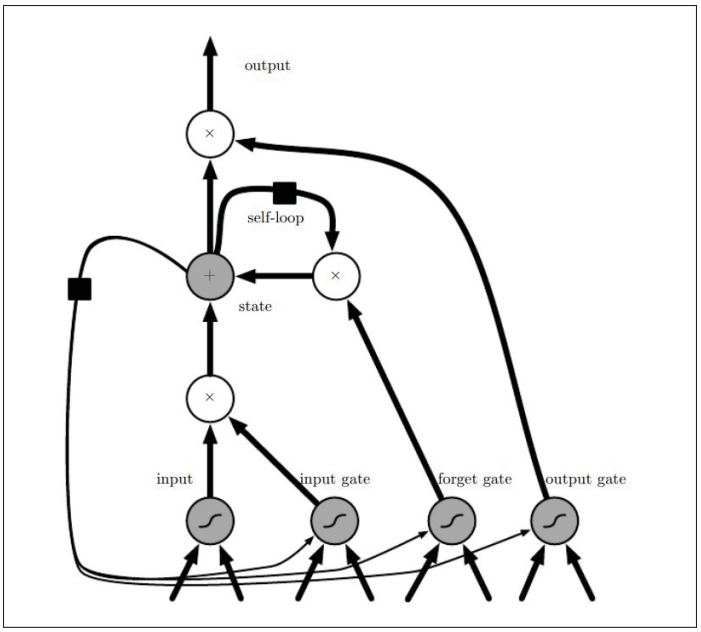

Figure 1.4 An example of an LSTM cell
Taken from Goodfellow *et al.* (2016)

In clinical practice, multiple EEG channels are recorded simultaneously from various scalp locations to compare the activity across different brain regions. The 1020 system for electrode placement in clinical EEG recordings has been recommended by the International Federation of Societies for Electroencephalography and Clinical Neurophysiology, as depicted in Figure 1.5 Rangayyan & Krishnan (2024).

Standard EEG instrumentation settings typically involve lowpass filtering at 75 Hz, with recordings at 100 $\mu V/cm$ and 30 mm/s, conducted over 8 to 16 simultaneous channels for a duration of 10 to 20 minutes. On the other hand, monitoring sleep EEG, for example to detect transients associated with epileptic seizures may necessitate multichannel EEG acquisition over several hours. Recording EEG signals during sleep is a part of polysomnography, which also includes the measurement of other physiological parameters such as eye movements, muscle activity, heart rate, and respiratory function to comprehensively assess sleep stages and identify sleep disorders Rangayyan & Krishnan (2024).

Extracted EEG signal during sleep is characterized by different brain waves, including Delta (0.1-4 Hz), Theta (4-8 Hz), Alpha (8-13 Hz), and Beta (13-30 Hz) Rangayyan & Krishnan (2024). Delta waves are associated with deep sleep and unconscious states, while Theta waves linked to drowsiness, light sleep and certain states of mediation. The alpha rhythm is the brain's primary resting rhythm, typically observed in wakeful, relaxed adults, particularly in the occipital region, and is characterized by bilateral synchrony. Auditory and mental arithmetic tasks performed with the eyes closed generate strong alpha waves, which are notably suppressed when the eyes are opened. High-frequency beta waves typically emerge as background activity in tense and anxious individuals. The depression or absence of the normal rhythm in a given state may indicate an abnormality. Figure 1.6 shows each brain wave corresponding to a specific frequency band Rangayyan & Krishnan (2024).

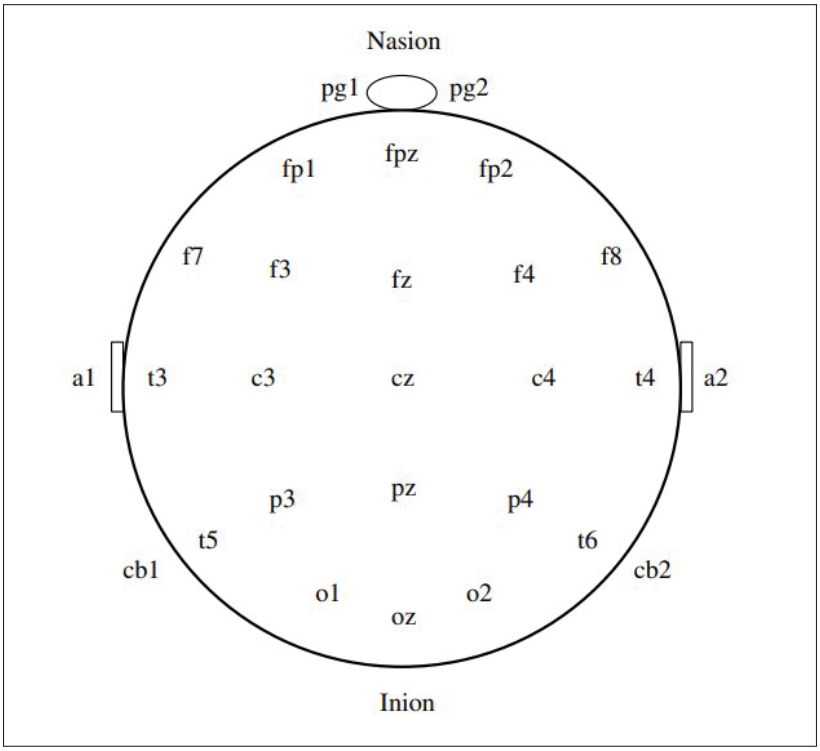

Figure 1.5 The 10-20 system of electrode placement for EEG recording
Taken from Rangayyan & Krishnan (2024)

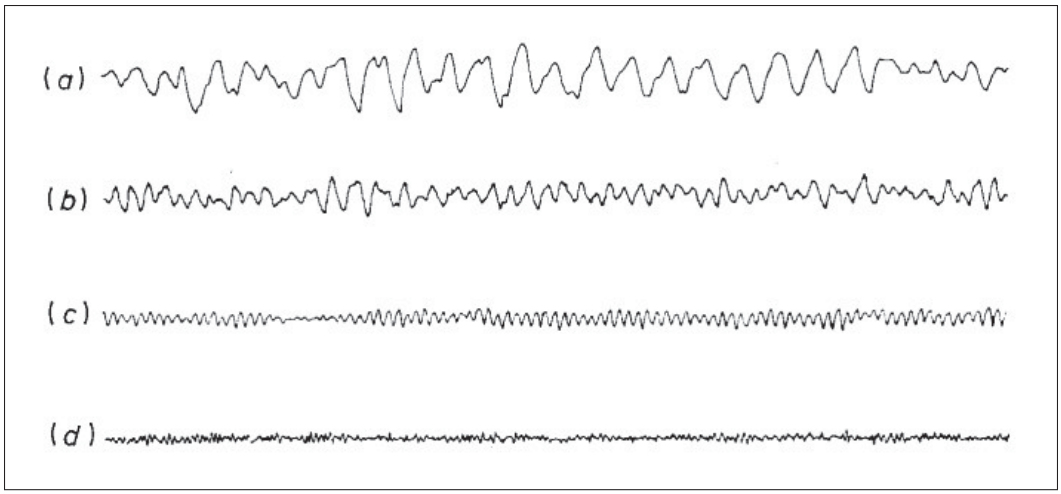

Figure 1.6 Brain waves: a) Delta wave b) Theta wave c) Alpha wave d) Beta wave
Taken from Rangayyan & Krishnan (2024)

1.1.3.2 Electrocardiogram (ECG)

The ECG represents the electrical activity associated with the heart's contraction and can be easily recorded using surface electrodes placed on the limbs or chest. In clinical practice, a standard 12-lead ECG is recorded using four limb leads and six chest leads. The right leg serves as the reference electrode, while the left arm, right arm, and left leg are used to obtain leads 1, 2, and 3, respectively Rangayyan & Krishnan (2024). A typical ECG waveform consists of the P wave, QRS complex, and T wave. P wave represents atrial contraction, QRS complex represents ventricular depolarization, and T wave represents ventricular repolarization. The schematic of a cardiac cycle with its segments is demonstrated in Figure 1.7. The ECG waveform can be altered by cardiovascular diseases and abnormalities, such as myocardial ischemia and infarction, ventricular hypertrophy, and conduction issues Rangayyan & Krishnan (2024).

The cardiac rhythm, or heart rate (HR), is regulated by specialized pacemaker cells found in the sinoatrial node, which is situated at the junction of the superior venacava and the right atrium Rangayyan & Krishnan (2024). HR is derived from the time intervals between successive R-peaks in the QRS complex and is calculated as the number of beats per minute (BPM). ECG

signal for HR monitoring usually uses a bandwidth of 0.5-50 Hz, which removes unwanted noises from the signal. The normal resting HR is approximately 70 BPM. While the HR decreases during sleep, an abnormally low rate below 60 BPM during activity may suggest a condition known as bradycardia. In contrast, The instantaneous HR can increase to as high as 200 BPM during intense exercise or athletic activity. A persistently high resting HR, which may be caused by illness, disease, or cardiac abnormalities, is known as tachycardia Rangayyan & Krishnan (2024).

Various methods are available for analyzing ECG signals to diagnose cardiac diseases, including hear rate variability (HRV) analysis in both time and frequency domains, as well as time-frequency domain analyses such as wavelet transform and STFT. However, this study focuses specifically on HR to detect depression, without delving into these other techniques.

1.2 Related Work

In this section, we review the existing literature on brain-heart interaction methods and explain various approaches that can capture the connection between these two important body systems. Additionally, we discuss the literature on depression detection using DL algorithms and review their performance as automated diagnostic tools for our classification task.

1.2.1 Existing Brain-Heart Interaction Methods in the Literature

Depression is a complex psychiatric disorder characterized by persistent low mood, reduced interest or pleasure in activities, a range of cognitive, emotional, and physical symptoms, and sleep difficulties. Its intricate interaction with both the central nervous system, particularly the brain's neurotransmitter systems, and the cardiovascular system, including potential links to inflammation and autonomic dysregulation, underscores the multidimensional nature of its pathophysiology Brandenberger *et al.*; Saad *et al.* (a).

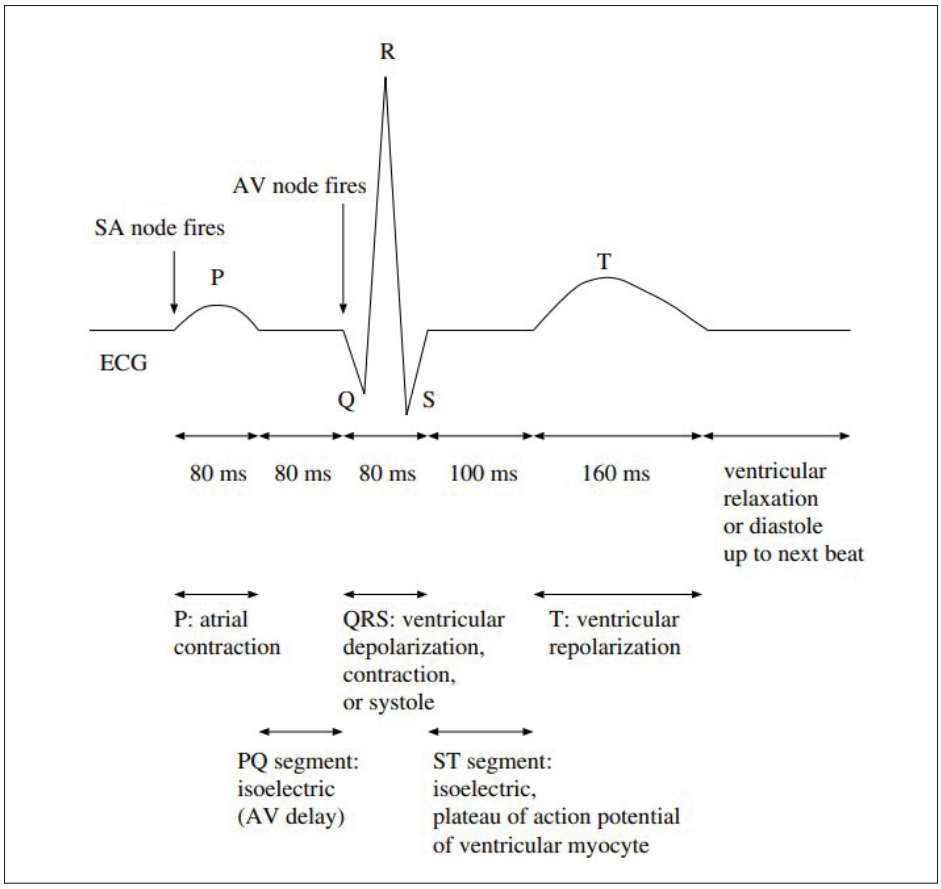

Figure 1.7 Schematic of a cardiac cycle with its segments
Taken from Rangayyan & Krishnan (2024)

According to recent studies Pinto & Parente, it is evident that major depression exhibits significant bio-markers within the cardiovascular and neurological systems. These biomarkers can serve as indicators to determine whether an individual suffers from this disorder.

Analyzing cardiac activity in individuals with and without depression can help identify key biomarkers. These biomarkers may include potential links to autonomic dysfunction, dysregulation of the hypothalamic-pituitary axis, increased HR, and reduced HRV during both wakefulness and sleep Saad *et al.* (b).

On the other hand, insights into depression can also be gained by studying the brain's neurological activities. These insights are drawn from EEG recordings and are generally considered to

be more reliable than traditional psychological questionnaires de Aguiar Neto & Rosa. A previous study de Aguiar Neto & Rosa, reveals that depression's primary biomarkers in EEG signals encompass various metrics, including multiple EEG band powers, evoked potential components, alpha asymmetry, signal characteristics, functional connectivity between various brain regions, and EEG vigilance. These biomarkers can help in distinguishing patients from healthy individuals.

Understanding how depression affects the cardiovascular and neurological systems separately can shed light on the interaction between these two related systems in detecting depression. Analyzing the patients' EEG and ECG signals in both the time and frequency domains could be highly effective in uncovering the interactions between these two systems. A previous study explored this interaction by analyzing the coherence between the power of the high-frequency (HF) component of HRV and the delta power band of the EEG signal in the C3 channel Jurysta *et al.* (a). This study showed that in individuals with depression, the coherence value, and the phase shift between the normalized power of HF and the power of the delta frequency band in EEG signal during sleep is similar to that of healthy individuals.

Various forms of interaction exist between two individual signals that allow us to assess their connection in terms of time, frequency, and time-frequency. Established methods enable us to depict the extent to which two specific signals are interconnected through their amplitude, phase, and frequency characteristics. These types of interconnection between two signals can be classified into six main categories: phase-to-phase coupling, phase-to-amplitude coupling, phase-to-frequency coupling, amplitude-to-amplitude coupling, amplitude-to-frequency coupling, and frequency-to-frequency coupling Jirsa & Müller (2013). To uncover these interactions, a detailed examination of each signal and an analysis of how each component of the signals interacts with one another are required. The following are some of the existing studies that utilize these coupling methods to explore interactions between brain and heart-related features.

Many studies have explored the relationship between the brain and heart by extracting features from raw EEG and ECG signals and analyzing their relationship. This exploration involves

uncovering connections between these signals. Since we are analyzing sleep data, it is important to note that it primarily comprises the lower frequency bands of the EEG signal. On the other hand, the ECG features under analysis primarily consist of HRV parameters, specifically focusing on HF, low frequency (LF), and very low frequency (VLF) parameters. These parameters are in the frequency ranges of 0.15-0.4Hz, 0.04-0.15Hz, and 0.015-0.04Hz, respectively Jurysta *et al.* (b).

For example, in a study conducted by Ako et al., the analysis involved calculating the power of the EEG in its respective frequency bands and HRV power-based parameters, including LF, HF, and LF/HF ratios, while considering different sleep stages in healthy participants Ako *et al.*. The study then examined the correlations between the mentioned time series and analyzed whether any significant correlations existed between them during each sleep stage. The study concluded that during the first three non-rapid eye movement (NREM) sleep stages, delta EEG shows negative correlations with LF and LF/HF. However, no correlation was observed between HF and EEG power in both rapid eye movement (REM) and NREM sleep, nor among the different NREM sleep stages.

Another study by Abdullah et al. focused on the interaction between the brain and heart, utilizing various synchronization metrics, including cross-correlation, mutual information (MI), and measures of nonlinear interdependence between EEG and ECG signals Abdullah, Maddage, Cosic & Cvetkovic (a). The study demonstrated a stronger interaction between these two signals during light sleep (specifically, NREM1 and NREM2) and REM sleep, as reflected in both linear and nonlinear interdependence indexes, compared to NREM3. This heightened interaction was linked to activity in the occipital brain region, leading to an increase in alpha activity and HR. In contrast, a study by Ehrhart et al. analyzed the relationship between EEG alpha activity and cardiac activity, finding an inverse relationship during REM sleep: alpha activity was low while HR was high Ehrhart *et al.*.

Two additional studies by Jurysta et al. and Brandenberger et al. focused on the connections between cardiac activity and the delta power of EEG Jurysta *et al.* (b), Brandenberger *et al.*. The

former specifically investigated the coherence between delta EEG and the HF component of HRV. The study demonstrated that individuals with sleep apnea-hypopnea syndrome exhibited lower coherence values during the first three cycles of NREM-REM sleep compared to individuals without the syndrome. Furthermore, no phase shift was observed between the HF and delta of EEG in both the control group and the group of patients with sleep apnea. On the other hand, Brandenberger et al. demonstrated an inverse coupling between delta activity and the $LF/(LF+HF)$ ratio during REM sleep and slow-wave sleep (SWS) stages Brandenberger *et al.*.

To comprehensively analyze the interaction between low-frequency EEG and HR, Rowe et al. investigated theta activity and HR in cats during REM sleep Rowe *et al.*. The study indicated that an increase in theta activity during this sleep stage could lead to an elevation in HR, suggesting a coupling between central activation of cardiac sympathetic nerves and theta wave oscillations.

In the context of phase synchronization, Jurysta et al. illustrated that cardiac vagal activity corresponds to HF activity preceding the delta oscillations Jurysta *et al.* (c). In another study, the phase of HR and various EEG frequency bands were used to calculate phase synchronization and directional coupling between the brain and the heart Abdullah, Maddage, Cvetkovic & Abdullah (b). The study concluded that, across most EEG frequency bands, individuals with sleep apnea had higher synchronization indices compared to healthy individuals. This synchronization generally decreased with deeper sleep stages, except during REM sleep. Additionally, the directional index revealed a predominant unidirectional coupling from the brain to the heart as EEG frequency increased.

Two studies assessed the coherence between EEG and ECG signals without feature extraction and analyzed the results for sleep apnea detection across various frequency ranges Khandoker, Karmakar & Palaniswami (b), Khandoker, Karmakar & Palaniswami (a). These studies found that in both the sleep apnea and healthy group, coherence between EEG and ECG is higher during REM sleep compared to NREM sleep stages across different frequency bands.

Given that most of the studies mentioned primarily examined amplitude-to-amplitude modulation—apart from those by Jurysta et al. and Abdullah et al.—our analysis will focus on this type of coupling, as it offers deeper insights into the relationship between the two signals.

1.2.2 Depression Detection with Machine Learning Algorithms

Recent progress in artificial intelligence offers the potential for supervised identification of depression. ML and DL algorithms learning from physiological signals, such as EEG and ECG, have significantly improved the discrimination of individuals with depression from control groups Mumtaz & Qayyum. These algorithms analyze signals recorded during wakefulness, capturing subjects' responses to various tasks or their resting state. This approach offers substantial improvements over traditional psychological questionnaires in terms of efficiency, requiring less time and effort, while also enhancing accuracy Zhang *et al.* (a). Consequently, ML and DL algorithms stand out as practical tools to help in the rapid and reliable diagnosis of depression.

More recently, the analysis and identification of mental disorders, including depression, have been increasingly informed by nocturnal sleep data Zhang *et al.* (b); Zhang *et al.* (a); Geng, An, Fu, Wang & An; Saad *et al.* (b); Moussa, Alzaabi & Khandoker. These data offer a unique glimpse into the baseline functions of the human body during rest, shedding light on patterns indicative of health and disease. Additionally, over 90% of individuals experiencing sleep disturbances are diagnosed with depression, which further emphasizes the relevance of utilizing sleep data for detecting and understanding this disorder Tsuno *et al.* (2005). Central to the mentioned studies is the use of polysomnography, which incorporates central and peripheral measurements such as EEG and ECG. In the context of EEG analysis, Zhang et al. extracted three features including PSD, symbolic transfer entropy (STE), and weighed phase lag index (WPLI) from sleep EEG channels Zhang *et al.* (b). Their research focused on brain functional connectivity, achieving optimal depression classification with minimal EEG channels (T3, T4, T5, T6) using a support vector machine (SVM) classifier. In another study, the same group extracted sleep stages and a combination of linear and non-linear features from two EEG channels

and an electrooculogram (EOG) channel and found that a random forest (RF) algorithm yielded the most accurate results in depression detection Zhang *et al.* (a).

In the context of ECG analysis, Geng et al. extracted time-frequency features of HRV from 5-minute segments of ECG signals recorded during sleep to classify depression Geng *et al.*. They developed a Bayesian-optimized extremely randomized trees classifier (BO-ERTC) to identify depression from the extracted features. Additionally, Saad et al. employed an HR profiling algorithm, incorporating HR and HRV parameters as inputs to a logistic regression algorithm with lasso regularization for the detection of depression Saad *et al.* (b). These approaches showed promise in depression classification using either EEG or ECG data.

Most existing sleep studies have focused on the potential of using either EEG or ECG alone for depression detection. Limited efforts have been made to integrate both central and peripheral signals, which are essential to fully understand the interconnections between these systems in the context of depression. One exception is a single study that assessed both EEG and ECG alongside breathing signals to identify depression in people with obstructive sleep apnea syndrome (OSAS) Moussa *et al.*. This research extracted 34 features for each 5-minute segment, consisting of the power of each channel, HRV parameters, and breathing-related features. Of the three classifiers used in this analysis, a 3-layer Multi-layer perception (MLP) exhibited the highest accuracy at 79.00%.

The mentioned studies leveraged statistical ML algorithms and employed feature extraction techniques to discern patterns indicative of depression Zhang *et al.* (b,a). However, handcrafted features often selected based on domain knowledge, may not fully capture the complex and subtle indicators of depression within sleep data. Additionally, some studies lack comprehensive validation procedures, which undermines the reliability and reproducibility of their findings. Saad *et al.* (b); Zhang *et al.* (b). The polysomnography recordings utilized in these studies span the entire night, typically lasting around 6 to 8 hours, and present a prolonged duration for analysis. The long volume of data is challenging to analyze and demands specialized algorithms to process effectively.

CHAPTER 2

UNVEILING HEART-BRAIN INTERACTIONS IN DEPRESSION: A COHERENCE ANALYSIS OF SLEEP EEG AND ECG

The results of this chapter were published and presented in the SLEEP 2024, the 38th annual meeting of the Associated Professional Sleep Societies in Houston, Texas.

2.1 Introduction

In this chapter, we concentrated on the most commonly studied form of coupling between the brain and heart signals in the literature—amplitude-to-amplitude coupling. We investigated the relationship between the brain and heart by directly analyzing EEG and ECG signals. We employed a dual measure called coherence that encapsulates the influence of both systems. This coherence measure is derived by calculating the CPSD of the two signals, assessing their correlation in the frequency domain.

To validate the coherence measurement results and thoroughly analyze the findings across various sleep stages and frequency bands, we applied a comprehensive statistical analysis. This approach considers all experimental results and assesses whether significant differences exist among them, helping to determine the nature of the brain-heart interaction between patients with depression and healthy individuals. To achieve this, we employed several statistical methods, including bootstrapping, t-tests, multiple comparison tests (MCT), and analysis of variance (ANOVA).

2.2 Methodology

2.2.1 Dataset

This study is based on secondary analysis of clinical data. It includes 86 cases: 46 diagnosed with MDD and 40 mentally healthy individuals. Polysomnography was recorded at the Royal Ottawa Mental Health Centre (ROMHC). This study was approved by the ethics committees

Table 2.1 Demographic information of the dataset

Group	# Cases	Sex (%male)	Age	BMI	Total Sleep Time (min)
MDD	46	30.61%	21±8.10	27±9.09	356.92±83.61
Control	40	44.89%	49±13.68	29±5.68	364.51±59.67

* All columns except the number of cases and sex have the format of $[Avg \pm SD]$

of ROMHC (Reference number: 2015028) and École de technologie supérieure (Reference number: H20221205). In this study, the depression status for each participant was determined based on medical records and confirmed using the Beck Depression Inventory (BDI-II), with a cutoff of $BDI - II \geq 14$ for the depression group and $BDI - II < 14$ for the healthy group INVENTORY-II (2010). Polysomnography recording included three EEG channels (F3, C3, and O1), ECG, chin and leg electromyogram, left and right electrooculogram, blood oxygen saturation, and respiratory efforts. The EEG and ECG channels that we utilized in this study were recorded with a sampling frequency of 256 Hz. Table 2.1 reports demographic characteristics for the MDD and control groups.

2.2.2 Preprocessing and Artifact Removal

EEG artifacts were automatically detected and removed using the method described by Coppieters't Wallant *et al.* (2016), which combines time- and frequency-domain analyses with adaptive thresholds. The pipeline includes modules for preprocessing, bad channel detection, feature extraction, and bad epoch detection. Bad channels—classified as noisy (e.g., due to poor contact) or flat (e.g., disconnected electrodes)—were identified based on abnormal standard deviation patterns. Artifacted epochs were detected in 1-second windows and included three main types: (1) popping artifacts, identified by rapid voltage transitions; (2) movement artifacts, flagged via elevated beta-band power linked to increased EMG activity; and (3) arousals, defined by transient shifts in EEG frequency lasting ≥3 seconds, coupled with a concurrent rise in EMG tone. This fully automated method enables robust and reproducible artifact rejection

across large-scale EEG datasets Lanthier *et al.*. In our study, we used a low-pass Butterworth filter on EEG signals to remove frequencies over 30 Hz, which are mostly high-frequency noise and do not provide much useful information for sleep data analysis. Epochs containing artifacts were excluded from the analysis.

ECG signal was filtered by a low-pass Butterworth filter with a cutoff frequency of 25 Hz. The mean of the signal was then subtracted to remove the baseline drift. To extract HR, the ECG signal was differentiated using a five-point derivative scheme to capture QRS slope information, followed by squaring the signal to emphasize higher frequencies. Next, a moving-window integration with a 32-sample window was applied to highlight the waveform features of the QRS complex. In the QRS detection stage, potential QRS complexes were identified by applying adaptive dual thresholds to both the window-integrated signal and the filtered ECG data, resulting in the detection of R-peak values. The stability of the RR intervals was ensured by comparing them against the averages of the last eight valid RR intervals. Any missed beats were identified and subsequently interpolated using cubic spline interpolation to maintain signal continuity Clifford & Tarassenko; Lázaro *et al.*.

The raw ECG and EEG signals during the pre-sleep and post-sleep periods were also discarded from the study due to the substantial presence of motion artifacts. We performed all artifact removal and noise reduction using Brainstorm and MATLAB. Details of our processing system configuration are provided in Table 2.2. The MATLAB and Python scripts used for preprocessing and implementation of the DL algorithms are available in the author's GitHub repository: https://github.com/mhazad99/Heart-Brain-Project.

2.2.3 Coherence Analysis

In this study, we selected a coherence metric, derived from cross-power spectral analysis of EEG and ECG signals, as the coupling biomarker. This metric captures brain-heart synchronization, which is linked to depression, allowing us to explore interactions between these systems for more effective detection.

Table 2.2 System configuration

Name	Parameter
OS	Ubuntu 18.04.5 LTS
GPUs	4 x RTX A6000 48GB
RAM	512GB DDR4
CPU	2 x Xeon Silver 4310 CPU @ 2.10GHz
Cores	24
MATLAB	R2022b
Python	3.11.8
Brainstorm	April 2023 version

The CPSD, which serves as a measure of the degree of coupling between EEG and ECG signals, is calculated as the Fourier transform of the cross-correlation between these two signals based on equation 2.1. In the equation 2.1, $x[n]$ = EEG and $y[n]$ = ECG.

To normalize this measurement between zero and one, a coherence metric was defined by dividing the absolute square of the CPSD value by the product of the power spectral densities of each signal, as follows:

$$C(f) = \frac{\left|S_{xy}(f)\right|^2}{S_{xx}(f)S_{yy}(f)} \tag{2.1}$$

where $C(f)$ is the coherence between two signals and S_{xx} and S_{yy} are the power spectral density of each signal.

Sleep stages were scored in 30-second epochs. For each 30-second epoch, EEG-ECG coherence values were calculated between the EEG channels (F3, C3, and O1) and the raw ECG signal with a hamming window length of 5120, and an overlap of 2560 samples. Coherence values were calculated separately for REM and NREM sleep stages. To mitigate power spectrum variance and provide a comprehensive measure of coherence, the calculated coherence values in the frequency domain were averaged across the entire night for each sleep stage and individual. The efficacy of this coherence metric is validated through analysis of variance (ANOVA) and multiple comparison tests (MCT), as presented in the results section.

2.2.4 Statistical Analysis

The statistical analysis in this chapter was divided into two parts. The first part involved a comprehensive bootstrapping method to ensure that the subsequent results were not due to chance. The second part assessed whether the coherence metric could significantly distinguish between healthy and depressed groups considering different sleep stages.

2.2.4.1 Bootstrapping Method

In this analysis, the average magnitude coherence (AMC) of each group was calculated and the difference between the AMC of these two groups was obtained as a baseline to evaluate its statistical significance, helping to determine whether the observed difference was due to chance.

To perform the bootstrapping method, it was necessary to define distinct clusters. This process involved setting a threshold to constrain the differences between the AMC of the two groups, thereby delineating the clusters. Subsequently, each segment exceeding the threshold was identified as a cluster. Various thresholds were tested based on p-value outcomes to identify the most distinctly separable clusters for this variation.

In the next step, it was essential to determine the optimal cluster representation, which would serve as the reference point for the subsequent t-test analysis. This optimal representation was a statistical feature of the data and could be defined in various ways, such as the maximum or minimum value within each cluster or the area under each cluster. In this study, we used the maximum value within each cluster as its representation. Figure 2.1 depicts the difference in coherence between the depression and healthy groups for the F3 channel. The threshold was set at 0.01, a value determined based on prior trials, to analyze all cluster frequencies exceeding this level. The maximum frequency for analysis was capped at 8 Hz. This choice reflected the primary focus of our study on lower frequencies during sleep and was also due to the fact that coherence differences did not yield distinguishable clusters at frequencies above this threshold.

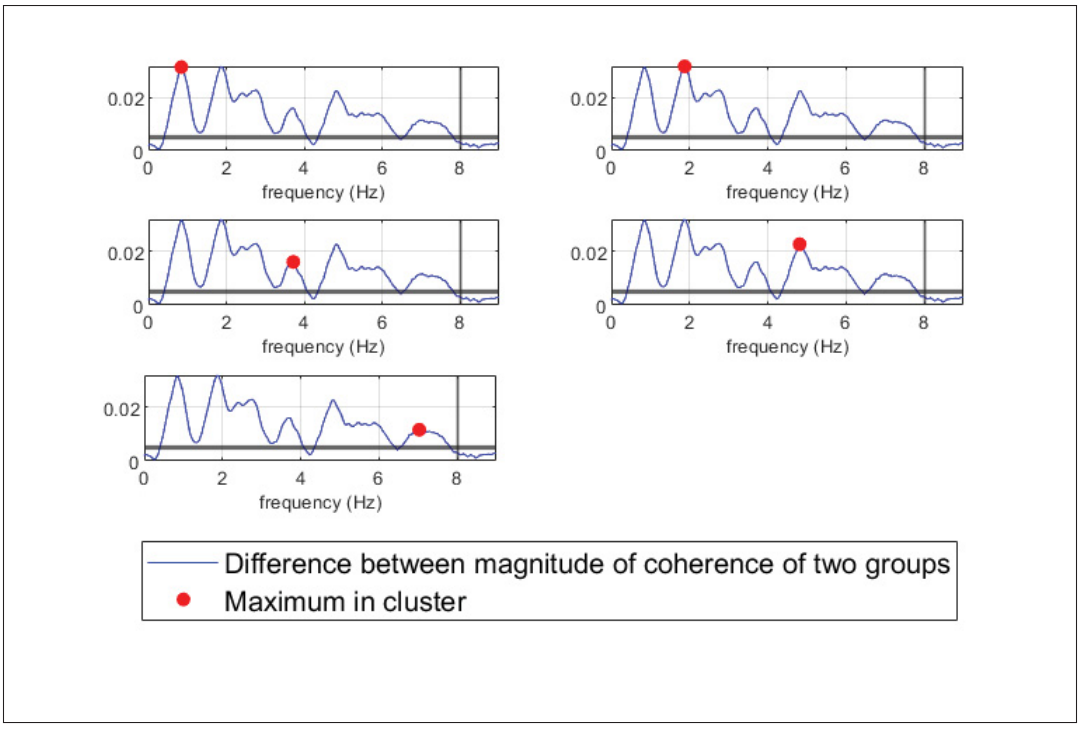

Figure 2.1 Difference between AMC of two groups in F3 channel. Red dots correspond to the maximum value in each cluster frequencies

The bootstrapping method, a statistical analysis technique, was mainly employed to assess the randomness of the coherence metric. This technique involves repetitive resampling from the observed data to estimate the sampling distribution of the statistic Gimenez-Nadal, Lafuente, Molina & Velilla. In this method, we generated two random groups by selecting 40 individuals each from both the control and depression groups. We then calculated the difference in AMC between the two newly formed groups and extracted the maximum value based on the specified thresholds. This procedure was repeated for 1000 iterations, and for each iteration, we collected the maximum value associated with the 0-8 Hz frequency cluster into an array. This resulted in an array with a length of 1000. Once we generated this array, we applied the t-test on each original cluster to determine if the mean of the generated array significantly deviated from the original clusters' maximum value. Figure 2.2 illustrates the distribution of maximum values that exceeded the 0.01 threshold within the 0-8 Hz range, as obtained from each bootstrapping iteration.

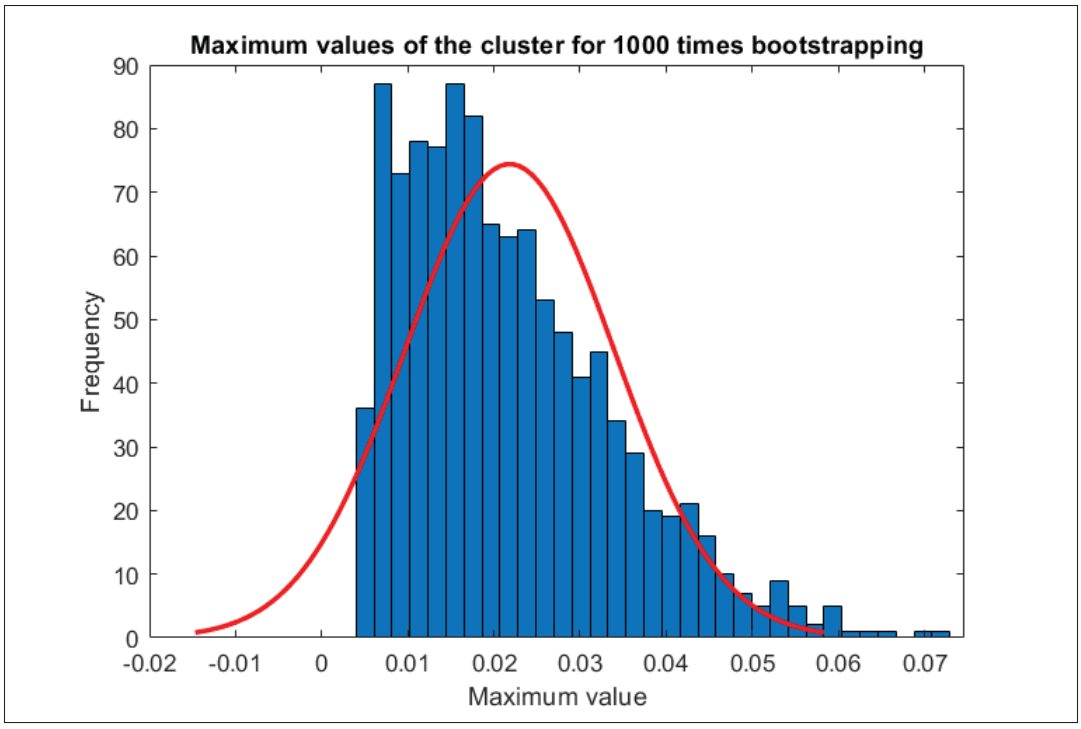

Figure 2.2 An example of the distribution of the cluster's maximum values after each bootstrapping

2.2.4.2 Significance Analysis of the Coherence Metric

In the next phase of the statistical analysis, we assessed the significance of the coherence metric as a distinguishing feature between healthy and depressed groups. To comprehensively assess EEG-ECG coherence throughout the night, we performed a detailed analysis separately for NREM and REM sleep stages, as well as for the entire night. The coherence values were calculated for NREM and REM sleep stages, along with the coherence between each EEG channel and the ECG signal, following the procedure previously described. To compare the coherence results across these sleep stages, we employed an ANOVA test in conjunction with an MCT. The MCT, an extension of the t-test designed for analyzing more than two groups, was used to further explore the differences.

2.3 Results and Discussion

2.3.1 Bootstrapping results

The results of the t-test, corresponding to the bootstrapping technique, are presented in Figure 2.3. It demonstrates that the coherence between the two groups is not due to chance and that there are significant differences between them. This confirms the validity of the results from the subsequent coherence analysis in this study. Figure 2.3 shows a significant difference in each cluster frequency between the EEG (F3) and ECG, with the exception of the fourth cluster, which does not reach significance at the 99% confidence level. The same result is observed for the C3 and O1 channels, providing evidence that the coherences across different frequency bands are not random.

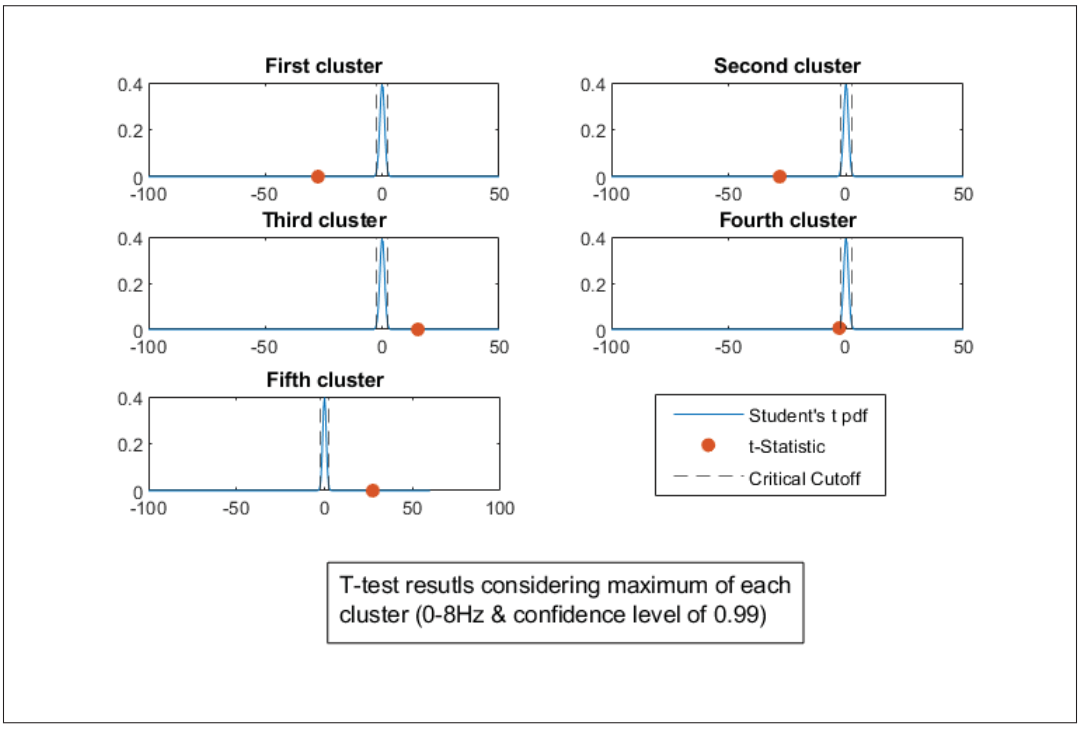

Figure 2.3 t-test results for the maximum values of each cluster in the bootstrapping method for the F3 channel

2.3.2 A Comprehensive MCT Analysis of Nighttime Coherence Across Sleep Stages in Healthy and Depressed Individuals

As depicted in Figure 2.4, preliminary results show that, in NREM sleep within the theta band, individuals with depression showed a significantly higher mean of EEG-ECG coherence values (MCV) compared to healthy controls across all EEG channels. MCVs for the depression and control group respectively were: 0.576±0.014 vs. 0.563±0.014 in F3, 0.545 ± 0.006 vs. 0.540±0.008 in C3, and 0.574±0.014 vs. 0.563±0.012 in O1 ($p<0.0001$). No significant group difference was observed during REM sleep. Furthermore, irrespective of depression status, the MCV in O1 was significantly higher in NREM compared to REM sleep for the full spectrum between the delta and theta bands ($p<0.00001$) as can be seen in Figure 2.4, 2.5. In contrast, MCV in F3 and C3 did not significantly differ between NREM and REM sleep. Figure 2.5 illustrates that in the delta band, regardless of depression status, the MCV was significantly lower in C3 compared to F3 and O1 during NREM sleep, but during REM sleep MCV was significantly higher in C3 than in O1 ($p<0.0001$).

2.4 Conclusion

This chapter primarily focused on evaluating a coherence metric to assess brain-heart interaction and determining whether this method effectively measures the connection between these two critical body systems. It can be concluded that the increased brain-heart coherence associated with theta activity during NREM sleep observed in individuals with depression may indicate more robust interactions between autonomic and cortical arousal systems. This could be one of the factors worsening sleep during depression. Beyond generating new insights about pathophysiological mechanisms underlying the high comorbidity between sleep, cardiovascular, and mental disorders, this may inform further work to identify multi-systemic biomarkers of depression.

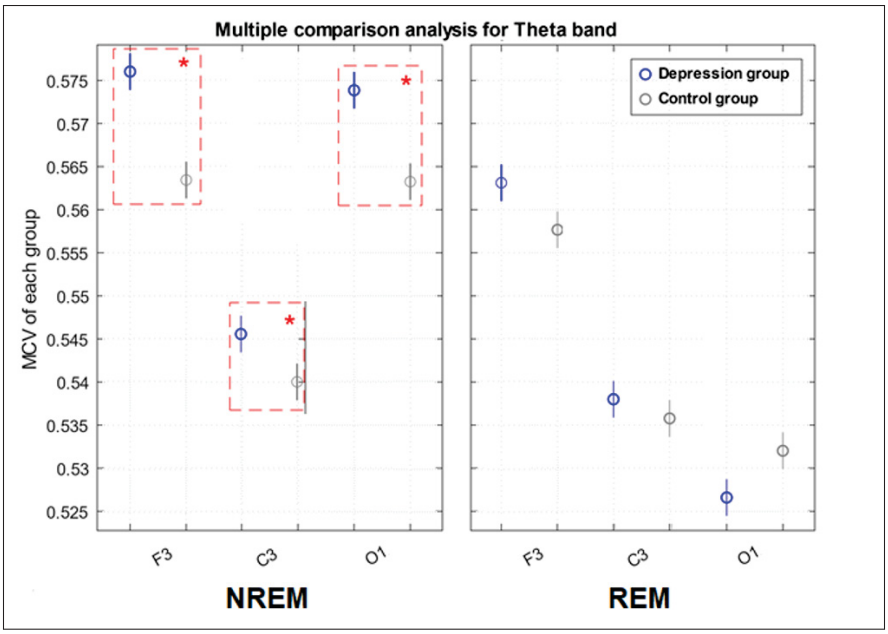

Figure 2.4 MCT was used to assess EEG-ECG coherence significance during REM and NREM sleep in the theta band. The blue circle and bar: Depression group, and The gray circle and bar: Control group. Note that if the bars for each group overlap, it suggests there is no significant difference between them. Conversely, if the bars do not overlap, it indicates a significant distinction between the groups

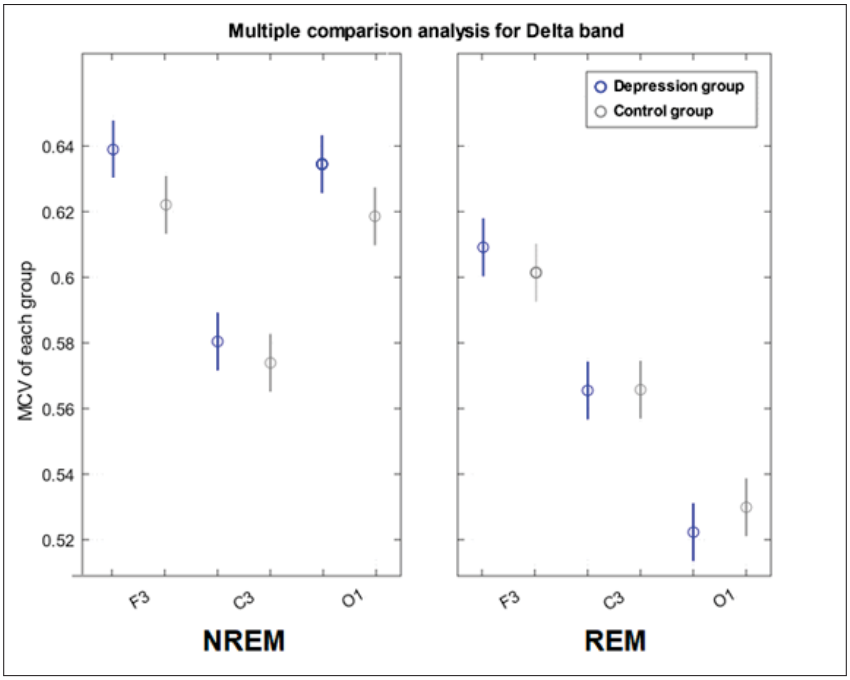

Figure 2.5 MCT was used to assess EEG-ECG coherence significance during REM and NREM sleep in the delta band

CHAPTER 3

SLEEPDEPNET: A MULTIMODAL RECURRENT-CONVOLUTIONAL NETWORK FOR DEPRESSION DETECTION USING SLEEP BRAIN-HEART BIOMARKERS

Mohammad Hasan Azad[1] , Rebecca Robillard[2,3] , Jean-Marc Lina[1] , Mohamad Forouzanfar[3]

[1] Department of Electrical Engineering, Ecole de technologie Supérieure, Montreal, Canada
[2] School of Psychology, University of Ottawa, Ottawa, Canada
[3] University of Ottawa Institute of Mental Health Research at the Royal, Ottawa, Canada
[4] Department of System Engineering, Ecole de technologie Supérieure, Montreal, Canada

Paper submitted for publication in the *IEEE Transaction on Biomedical Engineering*, December 2024.

3.1 Introduction

Major depressive disorder (MDD) is a prevalent condition that affects various aspects of life and is closely associated with sleep difficulties. Beyond the association of MDD with individual dysfunctions in the brain and heart, interconnected biomarkers bridging these critical physiological systems may facilitate objective MDD identification. Understanding and detecting these interrelations could provide valuable insights into identifying and managing this disorder Jurysta *et al.* (a).

The present study aims to develop a DL model for identifying depression by utilizing both independent and coupled information from various polysomnography channels. To this end, we introduce SleepDepNet, a specialized DL network designed to process distinct brain and heart depression biomarkers from polysomnography channels, as well as interrelated biomarkers between the brain and heart. Leveraging convolutional neural networks (CNNs) and long short-term memory (LSTM) networks, SleepDepNet adeptly captures intricate patterns and temporal dependencies within and across input channels. Additionally, the model incorporates distinct biomarkers linked to depression, seamlessly integrating them into the feature space to facilitate the final classification.

Drawing from recent research on depression biomarkers, we utilize the relative power ratio (RPR) of EEG delta, theta, alpha, and beta bands Wang *et al.*; Rangayyan & Krishnan (2024); de Aguiar Neto & Rosa, and HR derived from ECG Koch, Wilhelm, Salzmann, Rief & Euteneuer; Saad *et al.* (b) as primary inputs to our deep model. We also introduce a novel coherence metric between EEG and ECG signals to reflect brain-heart coupling, potentially offering deeper insights into the physiological mechanisms underlying depression. We thoroughly evaluate the performance of the proposed method on polysomnography recordings from 46 individuals diagnosed with depression and 40 healthy controls, spanning various age groups and both sexes, using a cross-validation technique.

The remainder of the paper is organized as follows: Section II delineates the methodology employed for our analysis, Section III presents the experimental results of the proposed method, Section IV deliberates on the results and compares them with existing literature, and the paper concludes in Section V.

A preliminary version of this work has been reported Azad, Robillard, Higginson, Lina & Forouzanfar.

3.2 Methodology

The preliminary sections of the methodology were outlined in Chapter 2 of the thesis. In this chapter, we start with the analysis of EEG and ECG data, followed by a detailed overview of the SleepDepNet architecture, which forms the core of the methodology.

3.2.1 EEG and ECG Analysis

Recent studies have identified several EEG-derived biomarkers as key indicators of depression, including different EEG band powers, alpha asymmetry, evoked potential components, and functional connectivity between various brain regions de Aguiar Neto & Rosa. Among these, the power of EEG in the delta, theta, and alpha frequency bands during sleep has been found to be particularly helpful for depression detection. Similarly, HR has emerged as an important ECG biomarker, with evidence showing elevated HR and decreased HRV are associated with

depression Koch *et al.*; Saad *et al.* (b). Based on these findings, we utilized HR derived from ECG and the RPR from EEG bands (delta, theta, alpha, beta) as primary inputs to our deep learning model.

HR signal was extracted from the ECG using the Pan-Tompkin algorithm as mentioned in the previous subsection with a sampling rate of 1 Hz among individuals Pan & Tompkins. Values exceeding 180 beats per minute (BPM) and falling below 40 BPM were considered outliers and were removed from the signal Tobaldini *et al.*. Ectopic beats were also eliminated from the HR using the Malik method Malik & Camm. These approaches resulted in a time series of the extracted HR signal for the entire night, which was ready for segmentation and feeding into the DL algorithm.

The RPR was derived from the power in the frequency bands of EEG channels, specifically the delta (0.5-4 Hz), theta (4-8 Hz), alpha (8-13 Hz), and beta (13-30 Hz) bands Wang *et al.*, as follows:

$$[D][T][A][B]RPR = \frac{BSP_{[\delta][\theta][\alpha][\beta]}}{BSP_{TotalPower}} \tag{3.1}$$

Here, BSP refers to band spectral power, calculated in 5-minute windows using the Welch method. The values within the brackets represent the RPR formula for the delta, theta, alpha, and beta frequency bands, respectively. This analysis extracted one value for RPR in each 5-minute window and resulted in a time series of RPRs for the entire night.

3.2.2 SleepDepNet

The architecture of the proposed SleepDepNet resembles that of a Siamese network, which is designed to process multiple inputs and evaluate the relationships between these inputs in the classification task Koochaki & Najafizadeh. Given that our dataset comprises long-duration one-dimensional time series data, we incorporated two main DL algorithms: 1-dimensional CNN (1D-CNN) and LSTM. 1D-CNN excels at capturing local patterns and features within the input channel, while LSTM captures long-term dependencies and maintains memory across

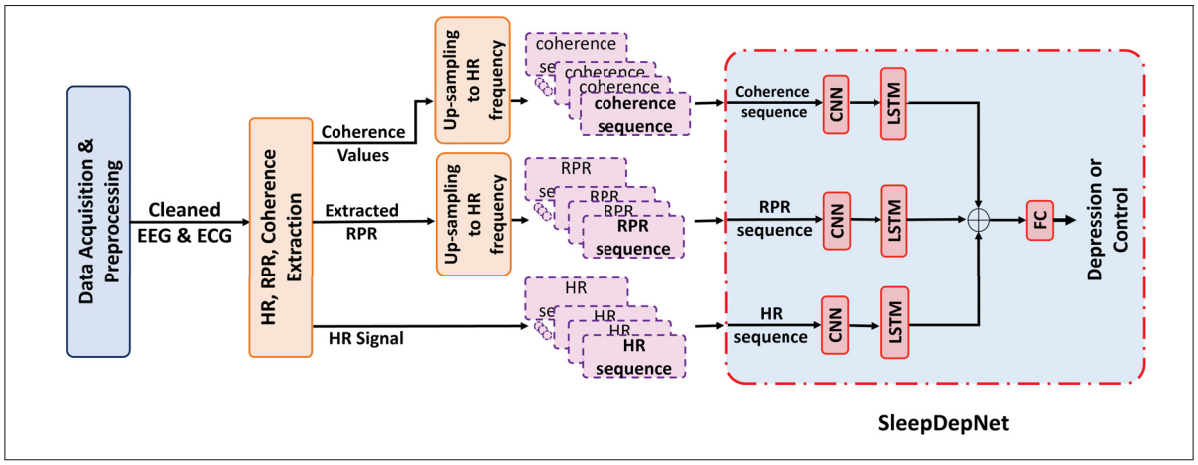

Figure 3.1 Overview of the SleepDepNet architecture for depression detection using brain and heart signals. This figure illustrates the data acquisition and preprocessing pipeline, including the extraction of HR, RPR, and coherence sequences. These sequences are upsampled to match the HR frequency and fed into the SleepDepNet model, which integrates CNNs for feature processing and LSTM networks for capturing temporal dependencies. The final fully connected layer classifies subjects into depression or control groups. HR: Heart Rate, RPR: Relative Power Ratio, CNN: Convolutional Neural Network, LSTM: Long-Short-Term Memory, FC: Fully Connected

time steps. Figure 3.1 provides an overview of the SleepDepNet architecture used in this study in detail in a block diagram.

1D-CNNs enable the precise extraction of locally significant features within each 1D signal. Their convolutional operations and hierarchical representations within convolutional layers empower the network to discern intricate patterns in the input data. Based on our hyperparameter optimization (see Section III), this study implemented a 1D-CNN architecture with three convolutional layers, each utilizing a kernel size of 3. Batch normalization, the ReLU activation function, and max pooling were incorporated after each convolutional layer to improve performance and mitigate overfitting. The batch normalization layer was used to improve the stability of training by mitigating the problem of vanishing gradients and reducing the dependence of gradients on the parameter scale. To add non-linearity to the network and enable it to learn complex relationships between input data, the ReLU activation function was used. Subsequently, the max pooling layer

with the kernel size and stride of three was employed to decrease the size of the feature maps, diminishing their spatial dimensions, while preserving the most significant features.

The input size of the 1D-CNNs was determined by the dimensions of the input signals: $T \times 1$ for HR, $T \times 12$ for RPR, and $T \times 3$ for coherence. Here, (T) represents the length of the time series, and the second element denotes the number of features in each signal type. The output of the 1D-CNN was then fed into an LSTM network for further processing.

The LSTM network was specifically designed for analysis of the sequential data. Since traditional recurrent neural networks often encounter the issue of vanishing gradients when processing long inputs, LSTMs were used. Our network architecture incorporates gating mechanisms that comprise input gates, forget gates, and output gates. These gates regulate the flow of information within the network, effectively addressing the vanishing gradient problem. Our LSTM network employs a dropout rate of 10%, which randomly deactivates a fraction of input units during training to prevent overfitting and improve generalization performance.

The input size of the LSTM network was set to 32, based on the number of CNN layers and their respective output lengths. The LSTM network used 16 hidden units to capture abstract representations and temporal dependencies in input data. Four critical hyperparameters—number of LSTM layers, number of hidden units, dropout rate, and sequence length—were determined through cross-validation (see Section III). During training, the initial hidden and cell states for each element in the input sequence were randomly initialized.

To find the combined effect of all three input types (HR, RPR, and coherence) on the final depression classification, the last hidden layer activations from each SleepDepNet branch (corresponding to each input type) were extracted and concatenated. This concatenated matrix was then passed through three fully connected layers, each using the ReLU activation function and a 10% dropout rate. The final fully connected layer employed a Softmax function to normalize the output into probabilities for the two-class classification task (depressed or non-depressed).

In the training steps, the adaptive moment estimation (ADAM) optimization algorithm was used. This algorithm converges faster than the traditional stochastic gradient descent algorithm since it adjusts the learning rate dynamically through the learning process. The value for hyperparameters was fixed after applying the nested cross-validation approach. To minimize the error in binary classification, we utilized the cross-entropy loss (CE) function as follows:

$$CE = -\frac{1}{N}\sum_{i=1}^{N}[y_{i1}log(\hat{y}_{i1})) + y_{i2}log(\hat{y}_{i2}))] \tag{3.2}$$

where N is the number of samples, y_{ij} is an indicator function that is 1 if sample i belongs to class j, and 0 otherwise, and $\hat{y}_{ij}$ is the predicted probability that sample i belongs to class j. This loss function quantifies the dissimilarity between the actual labels and the predicted ones. It imposes a greater penalty on incorrect predictions compared to correct ones, rendering it particularly suitable for classification tasks where accuracy is important. Besides, to prevent overfitting, regularization techniques were employed. Specifically, L1 and L2 regularization parameters were incorporated into the loss function. These parameters were adjusted when the validation loss was not decreasing, even as the training loss continued to decrease.

In addition to our hybrid architecture, we implemented a basic CNN and a CNN-LSTM network, considering different input information. This allowed us to evaluate the performance of SleepDepNet in comparison to basic networks.

To prepare the inputs for our SleepDepNet multi-head network and to capture temporal dependencies, we preprocessed HR, and RPR as mentioned in the methodology. For the coherence metric, we focused on the lower frequency range (4-8 Hz) based on the statistical results of the coherence analysis. Coherence values within this frequency band were calculated in 5-minute windows irrespective of sleep stages and averaged across the night, producing a sequence of coherence samples in the frequency domain that reflects the evolution of neural-cardiac synchrony during sleep. To feed these inputs to the network, we needed to ensure that all input signals had the same length. To achieve this alignment, we upsampled the extracted

RPR and coherence values using linear interpolation so they matched the size of the HR signals. This critical preprocessing technique adjusted all input channels (HR, RPR, and coherence) into the sequences of data with equal length. After this step, we segmented the entire data into sequences of 60 seconds each, with the sequence length being a chosen hyperparameter. Each segment was labeled to indicate whether it belonged to the control or the depression group. These standardized sequences were then fed into the SleepDepNet model, enabling it to effectively learn and leverage the temporal relationships within and across the different physiological signals.

3.3 Experimental Results

In this section, We report the results of depression classification using our SleepDepNet and compare them with other existing DL algorithms in this application to assess the efficacy of our proposed method.

We employed a nested cross-validation approach with 10 outer loops each having 5 inner loops to validate our classification algorithm. Prior to cross-validation, all subjects—both healthy controls and MDD patients—were divided into two distinct, non-overlapping groups corresponding to training-validation, and test sets, ensuring that each subject appeared in only one of these sets throughout the entire process. The entire dataset was divided into 10 folds, where one fold was taken as the test set (10% of the data) and the others were taken as the training-validation set (90% of the data). This strict, subject-level split eliminated any possibility of data leakage—no data from a participant in the test set were ever used for training or validation. In each outer loop, the training-validation set was further divided into 5 inner folds, where one fold was used for validation and the rest were used for training the model. This process was repeated 5 times, ensuring each fold served as a validation set once. In each inner loop, the model was trained on the training folds and validated on the validation fold. Then we selected the best hyperparameters based on performance across all of the validation sets. Finally, with the best hyperparameters identified, the model was trained on the entire training-validation set (90%) in each outer loop and evaluated on the test set (10%) of that outer loop. Because the numbers of healthy and MDD

Table 3.1 Best Hyperparameters of SleepDepNet after Cross-validation

Hyperparameter	Searching space	Selected
# CNN layers	{3, 4}	3
CNN kernel size	{3, 5}	3
Batch size	{64, 128, 256, 512}	128
Learning rate	{0.0001, 0.001, 0.01}	0.001
Dropout rate	{0, 0.1, 0.2, 0.3}	0.1
# LSTM layers	{2, 3, 4, 5}	2
# LSTM hidden layers	{16, 32}	16
LSTM sequence length	{30s, 60s, 120s, 180s}	60
# fully connected layers	{2, 3}	3

subjects were approximately equal, every fold remained class-balanced, ensuring a fair binary classification task. Table 3.1 presents the best hyperparameters of our network determined through majority voting from all outer loops. The final results were obtained by averaging the performance metric of the test sets across all 10 outer loop iterations.

The same validation method was applied to tune the hyperparameters of the CNN and CNN-LSTM networks, resulting in their best outcomes presented in Table 3.2.

Table 3.2 summarizes the results in terms of the accuracy, precision, recall, and F1-score for different models being analyzed on the unseen test data.

Our findings summarized in Table 3.2 demonstrate that using HR information with a CNN architecture achieves superior performance compared to using RPR. The CNN with HR yielded accuracy, precision, recall, and F1-score of 80.43%, 81.22%, 80.48%, and 80.47%, respectively, whereas RPR resulted in significantly lower scores (74.09%, 75.25%, 64.37%, and 67.75%). Furthermore, our results revealed that switching to a CNN-LSTM architecture and using HR as input leads to an improvement of approximately 2% across all evaluation metrics compared to CNN alone. The most promising results were achieved with the SleepDepNet architecture, which integrates HR, RPR, and the coherence metric as inputs, and combines CNN and LSTM

Table 3.2 Performance of Different Networks with Corresponding Inputs

Methods-[Inputs]	Accuracy	Precision	Recall	F1-score
SVM-[Coherence]	53.32%	52.54%	53.58%	53.01%
1DCNN-[Coherence]	55.83%	56.29%	55.08%	55.61%
SleepDepNet-[Coherence]	61.41%	61.80%	61.11%	61.42%
CNN-[HR]	80.43%	81.22%	80.48%	80.47%
CNN-[RPR]	74.09%	75.25%	64.37%	67.75%
CNN-LSTM-[HR]	82.15%	83.32%	81.40%	82.18%
CNN-LSTM-[RPR]	74.28%	71.89%	64.44%	65.98%
SleepDepNet-[HR-RPR]	97.13%	98.39%	97.30%	97.82%
SleepDepNet-[HR-RPR-Coherence]	**98.33%**	**98.10%**	**98.61%**	**98.34%**

layers. This technique resulted in the highest performance within the SleepDepNet framework: accuracy of 98.33%, precision of 98.10%, recall of 98.61%, and f1-score of 98.34%.

3.4 Discussion

Depression has far-reaching implications for health, daily functioning and well-being. Our research explored the intricate relationship between cardiac and cortical activity during sleep, providing valuable insights into some of the physiological underpinnings of depression. SleepDepNet, a novel deep learning framework, showcased the potential of advanced analytical techniques in this domain. By integrating time series data from multiple heart and brain biomarkers through CNN and LSTM architectures, SleepDepNet effectively extracted and fused multi-systemic information embedded in time-dependent features of sleep physiology. This innovative approach achieved a classification accuracy of 98.33%, demonstrating the feasibility of leveraging sleep data analysis for depression identification and highlighting the need for further refinement and testing to enhance its clinical applicability.

In this study, we focused on three input types for our model: HR (extracted from ECG) as a heart biomarker, theta RPR (extracted from EEG) as a brain biomarker, and an EEG-ECG coherence metric as a brain-heart coupling biomarker. The flexibility of our proposed multi-

head architecture allows for the seamless integration of additional input data from various polysomnography channels, as well as the exploration of different coupling biomarkers. The choice of the window size for calculating RPR and coherence values was based on RPR analysis. We tested 2, 5, and 10-minute windows for RPR calculation and found that 5-minute windows yielded the best results for the CNN and CNN-LSTM networks. The accuracies for 2, 5, and 10-minute windows of RPR for CNN and CNN-LSTM were 71.01%, 74.09%, 68.33%, 73.59%, 74.28%, and 73.33%, respectively. This suggests that a 5-minute window provides an optimal balance between sufficient data for reliable feature extraction and maintaining temporal resolution to capture meaningful physiological changes during sleep. Based on these results, we used 5-minute windows in our network design.

We conducted extensive experiments to compare the performance of individual biomarkers across various network architectures and their combinations. Our classification results suggest that HR may be a more powerful biomarker for depression classification than RPR in the theta range, particularly when used with a CNN-LSTM architecture as shown in Table 3.2. Several factors may contribute to a superior performance of HR. Depression profoundly affects the autonomic nervous system, which is intricately linked to cardiac function, making ECG biomarkers particularly sensitive to physiological changes associated with depression Thayer & Lane. Additionally, ECG signals generally exhibit greater robustness and clearer patterns with less susceptibility to noise compared to EEG signals Licht *et al.*. This inherent signal quality may facilitate more accurate analysis by DL algorithms. Importantly, we utilized EEG data from frontal, central, and occipital regions, but did not incorporate data from other crucial areas like the temporal and prefrontal regions. Recent research suggests these regions may play an even more significant role in depression detection Zhang *et al.* (b). Integrating data from these additional EEG channels could potentially enhance the classification accuracy of future models.

Beyond analyzing individual EEG and ECG data, we developed a novel coherence metric to capture the coupling between these signals. Several approaches exist for coupling analysis, involving the examination of the amplitude, phase, frequency, and information flow of two signals to reveal the extent of their connectivity Jirsa & Müller (2013); Catrambone & Valenza.

Since the power of EEG and ECG signals contains crucial information about depression, our study specifically focused on extracting the amplitude-to-amplitude modulation between EEG and ECG signals de Aguiar Neto & Rosa; Saad *et al.* (b). Among various techniques for measuring amplitude-to-amplitude modulations between two signals, CPSD stands out because it provides frequency and phase domain information about the relationship between two signals. Moreover, it can be efficiently calculated using the Fast Fourier Transform algorithm, making it computationally feasible for analyzing large datasets.

The coherence metric, particularly within the theta frequency band, proved to be a significant factor in differentiating between depression and mentally healthy states. This finding aligns with the established role of theta activity in depression classification Goldschmied, Cheng, Armitage & Deldin. Of note, abnormalities in the coherence metric extend beyond depression. Two prior studies utilizing raw EEG and ECG signals to calculate coherence reported similar results regarding sleep apnea detection Khandoker *et al.* (b,a). These studies observed significant differences in EEG-ECG coherence between healthy individuals and individuals with sleep apnea across various sleep stages and frequency bands. Future studies are thus required to assess the specificity of EEG-ECG coherence profiles to depression.

Although Fig. 2 highlights a significant group-level difference in theta-band coherence between control and depression subjects during NREM and REM stages, our classification experiments using only coherence as input reveal its limitations as a standalone feature. Specifically, when coherence was used alone, SleepDepNet achieved an accuracy of 61.41%, while a 1D-CNN and SVM reached only 55.83% and 53.32%, respectively. These results indicate two key insights. First, despite its statistical significance at the group level, coherence lacks sufficient discriminative power on its own for subject-level classification across a full night's recording. Second, coherence compresses EEG–ECG dynamics into short temporal windows, thereby discarding long-range temporal dependencies that are critical in depression detection over the course of sleep (6–8 hours). Additionally, the lower performance of conventional classifiers like SVM suggests that DL is better suited for capturing subtle and temporally distributed patterns across multimodal sleep data.

Table 3.3 Comparison with Related Literature

Literature	Dataset	Algorithm & Feature	Results	Limitations
Zhang *et al.* (b)	Sleep EEG (T3,T4,T5,T6) 30 healthy, 30 depression	SVM WPLI, STE features	Acc: 99.61% Pre: 99.49% Rec: 99.62%	- Train-test ratio ignored - Hyperparameter selection missed - Limited age group
Zhang *et al.* (a)	Sleep EEG (C3,O1) and EOG 20 healthy, 20 depression	RF 16 linear/non-linear features	Acc: 94.56%	- High computational cost
Geng *et al.*	Sleep ECG 40 healthy, 40 depression	BO-ERTC 24 HRV features time-frequency	Acc: 86.32% Pre: 85.48% Rec: 91.45%	- HR not input - Feature ranking expensive
Saad *et al.* (b)	Sleep ECG 529 healthy, 664 depression	Logistic regression HR, HRV	Acc: 79.90% Rec: 82.80%	- Method details missing
Moussa *et al.*	Sleep ECG, EEG, breathing 40 OSAS, 40 OSAS with depression	3-MLP 34 features	Acc: 79.00% Pre: 80.30%	- ECG features not used - Other DL algorithms not explored
This study	Sleep ECG, EEG (C3,F3,O1) 40 healthy, 46 depression	SleepDepNet 3 features (HR, RPR, coherence)	**Acc: 98.33%** **Pre: 98.10%** **Rec: 98.61%**	- Limited sample size - Other brain-heart biomarkers not explored

Although CNN-LSTM outperformed other methods on its own, the highest overall accuracy (98.33%) was achieved by our SleepDepNet model, which integrates HR, RPR, and the coherence metric. This emphasizes the significant value of the network's architecture and components, including the coherence metric and upsampling of the input data in the depression classification task. Notably, integrating coherence values as an additional input enhanced the network's accuracy by approximately 1.5%, highlighting its considerable impact. Moreover, when integrating multiple biomarkers with different sampling resolutions, it is essential to align them to the same resolution within our network. Upsampling the RPR and coherence values to match the higher frequency of HR data led to a significant 13% improvement in final accuracy compared to downsampling HR. This process enriched the network with additional information, enhancing its training and overall performance within the SleepDepNet framework.

Table 3.3 compares our results to that of previous similar studies. The highest accuracy (99.61%) was achieved by a study focusing on the brain's functional connectivity during sleep, which employed specific features such as PSD, WPLI, and STE Zhang *et al.* (b). However, this study did not specify the details of their train-test split, leaving uncertainty about the proportion of data used for training and testing. Additionally, there is no mention of a validation set or

cross-validation, raising concerns about the determination and validation of hyperparameters in the ML algorithm.

Zhang B. et al.'s inclusion of sleep stages in their analysis supports our coherence analysis results, indicating that brain-heart coherence during NREM sleep is more effective than during REM sleep in discriminating depression Zhang *et al.* (a). On the other hand, the computational expense of the combination learning used in this study is notable, considering it calculates the combination of all possible 240 features, classification algorithms, and sleep stages.

In the case of depression classification using sleep ECG signals, Geng et al. focused on extracting HRV parameters and employed computationally expensive feature importance methods, such as mean impurity reduction and permutation-based feature importance, achieving an accuracy of 86.32% Geng *et al.*. The utilized ranked feature importance methods are computationally expensive because they require multiple evaluations of the model after modifying or permuting features. To manage this complexity, Geng et al. applied the ranked feature importance method exclusively to the test set to minimize the computational burden. In contrast, our approach bypasses the need for HRV feature extraction, allowing the network to classify individuals based solely on HR, enabling a more efficient and streamlined model for depression detection with greater accuracy.

The dataset utilized in our analysis is a subset of the Saad et al. dataset, which included a larger number of participants, making its results more robust Saad *et al.* (b). Nevertheless, SleepDepNet demonstrated significantly higher accuracy compared to the results reported in Saad et al. Future work will aim to extend our current methods to larger datasets.

Moussa et al. conducted the only study to date that considered both sleep EEG and ECG signals for depression analysis, achieving an accuracy of 79.00% Moussa *et al.*. After feature ranking, they determined that EEG features alone including the power of theta, alpha, and beta bands in F3, and F4 channels were sufficient for their final classification, without the need for additional ECG features. The utilized Chi-square analysis revealed that the ECG features used, such as the power of HR in the VLF, LF, and HF frequency bands, were not sufficiently informative for

detecting depression. As a result, these features were excluded prior to being input into the ML and DL algorithms for classification. However, this approach may have overlooked potential benefits of combining both signals. In contrast, our DL analysis incorporates both EEG and ECG data, leveraging the temporal dynamics of HR, providing a more comprehensive method for depression classification.

Unlike previous studies, we prioritized the development of an automated framework combining brain and heart biomarkers for depression detection from sleep data. We employed DL algorithms to go beyond simple feature extraction, focusing on the complex interactions between these combined inputs. Our proposed network has the potential to be adapted for other conditions linked to mental health or sleep, including other types of affective disorders, sleep apnea, and insomnia. Its flexibility allows for the integration of various polysomnography signals (e.g., EOG, EMG), significantly broadening its applicability. Naturally, this research has some limitations. With a limited dataset, we plan to explore additional inputs and how they impact results with a larger sample size. We also intend to investigate other interconnected brain-heart biomarkers derived from signal characteristics such as mutual information and various types of coupling between the two signals, with the potential to improve detection accuracy. Additionally, we will explore other advanced DL algorithms designed for time series classification as a way to potentially refine our depression detection application.

Overall, this study establishes a strong foundation by analyzing both central and cardiac signals, alone and in combination, strengthening the notion that they represent important components of the pathophysiology of depression – an area with significant room for further exploration.

3.5 Conclusion

This study developped SleepDepNet, an automated DL framework for depression identification from sleep data using both independent and coupled brain-heart biomarkers. The framework seamlessly integrates independent brain and heart biomarkers (EEG RPR and ECG HR), as well as a novel brain-heart coupling index derived from EEG-ECG coherence. The coherence metric

proved to be helpful in distinguishing between people with depression and mentally healthy controls, emphasizing its potential as a reliable feature for enhanced classification. However, the combination of this metric with HR and theta activity was found to have a better classification value than the individual metrics. SleepDepNet's architecture, composed of CNN and LSTM layers, effectively captures relevant features and temporal dependencies within these biomarkers. Through extensive experimentation with various input combinations and architectures, we found that combining RPR, HR, and the coherence metric yielded the highest depression identification accuracy (98.33%). While this study focused on specific biomarkers, SleepDepNet's modular design inherently allows for the incorporation of additional biomarkers from other bodily systems or further exploration of brain and heart measures. Our proposed framework offers a new avenue for combining diverse physiological data to achieve a more comprehensive characterization of depression. Future work will focus on expanding the dataset, notably to assess diagnostic specificity, and refining the model to improve diagnostic accuracy and clinical utility.

CONCLUSION AND RECOMMENDATIONS

4.1 Summary

In this dissertation, we developed a pipeline for detecting depression by analyzing brain-heart biomarkers. We demonstrated that these biomarkers can be independent of each other, with brain-related biomarkers such as EEG frequency band power and heart-related biomarkers like HR each contributing to the detection process. Moreover, we demonstrated that coherence between brain and heart activity serves as a coupling biomarker for depression. This metric can effectively differentiate between depressed and healthy individuals within specific frequency bands and sleep stages.

In the first chapter, we established the foundational background by explaining essential definitions and concepts that are crucial for understanding the subsequent chapters of the thesis. Subsequently, we conducted two comprehensive literature reviews. The first review focused on existing methods in the literature that explore brain-heart interactions in sleep data. These methods employed various approaches to analyze the interactions between EEG and ECG signals, either by using the raw signals directly as inputs or by extracting specific features from the signals to examine their relationships in both time and frequency domains. Secondly, we reviewed the existing literature on studies that employed sleep EEG and ECG signals, along with their variations, as inputs to machine learning algorithms for classifying groups as either depressed or healthy.

In the second chapter, we introduced the dataset used for our analysis and detailed the preprocessing techniques required to prepare the data for subsequent steps. We then delved into the coherence metric, evaluating its potential as an effective brain-heart biomarker capable of significantly distinguishing healthy individuals from those with depression. To validate the effectiveness of this metric, we conducted several statistical tests, including bootstrapping, t-tests, ANOVA, and MCT. The results from these analyses demonstrated that the MCV is

significantly higher in depressed individuals compared to healthy controls, particularly within the theta frequency band and all EEG channels during NREM sleep stages. The MCV values for the F3 channel were 0.576 ± 0.014 for the depression group and 0.563 ± 0.014 for the control group. For the C3 channel, the values were 0.545 ± 0.006 for depression and 0.540 ± 0.008 for control. In the O1 channel, the results were 0.574 ± 0.014 for the depression group and 0.563 ± 0.012 for the control group, with a p-value < 0.0001. This finding suggests that coherence could serve as an important interrelated brain-heart biomarker for depression detection.

In the final chapter, we introduced a fully automated DL algorithm for depression detection, named SleepDepNet. This network utilizes RPR, HR, and coherence values as inputs. The architecture of SleepDepNet combines CNNs and LSTM networks. The CNN component is mainly responsible for extracting critical features from the input data, while the LSTM component captures the temporal dependencies within the data, leading to a more robust classification of the cases. Another crucial aspect of the proposed network is the concatenation of the data at a specific stage, which integrates all the information from the various inputs. This fusion of data enhances the network's ability to make an accurate final classification. The SleepDepNet demonstrated a high classification accuracy, precision, recall, and F1-score of 98.33%, 98.10%, 98.61%, and 98.34% using the three aforementioned inputs, respectively. When compared to other studies in the literature, the results of our proposed SleepDepNet network proved to be highly reliable, suggesting that it could serve as a comprehensive pipeline for the detection of depression and potentially other mental health disorders.

4.2 Future Work

This research holds significant potential for future studies. The dataset used was a subset of a larger dataset, which can be leveraged in subsequent studies to enhance the robustness of our model. Utilizing the full dataset will facilitate more comprehensive training, validation, and testing, potentially improving the model's performance with a larger volume of data. Additionally,

the dataset used was private and relatively unexplored, which made it challenging to compare our findings with existing literature. Applying this method to an open-source dataset would allow for a more robust comparison with other studies, providing a fairer and broader evaluation of our results.

Furthermore, the analysis of existing brain-heart biomarkers for depression should be expanded, as there are numerous metrics and interactions between these critical body systems that remain to be explored. In this research, we only focused on one aspect within these systems to identify coherence as an effective biomarker. However, other interrelated biomarkers may still need to be discovered and investigated in future work.

Artificial intelligence is rapidly advancing, enabling the development of increasingly accurate and reliable networks and methods. The network introduced in this research was meticulously designed to classify physiological data for the detection of mental health disorders with high accuracy. However, it is important to recognize that there are numerous other network designs and modifications that could further enhance performance. Exploring and experimenting with new and state-of-the-art DL algorithms and techniques may lead to even better results in this area.

BIBLIOGRAPHY

Abdullah, H., Maddage, N., Cosic, I. & Cvetkovic, D. Brain and heart interaction during sleep in the healthy and sleep apnoea. *2010 IEEE EMBS Conference on Biomedical Engineering and Sciences (IECBES)*, pp. 276–280. doi: 10.1109/IECBES.2010.5742243.

Abdullah, H., Maddage, N., Cvetkovic, D. & Abdullah, H. Phase synchronization and directional coupling between brain and heart during sleep. *2012 IEEE-EMBS Conference on Biomedical Engineering and Sciences*, pp. 659–663. doi: 10.1109/IECBES.2012.6498075.

Ako, M., Kawara, T., Uchida, S., Miyazaki, S., Nishihara, K., Mukai, J., Hirao, K., Ako, J. & Okubo, Y. Correlation between electroencephalography and heart rate variability during sleep. 57(1), 59–65. doi: 10.1046/j.1440-1819.2003.01080.x.

Azad, M. H., Robillard, R., Higginson, C., Lina, J.-M. & Forouzanfar, M. 0960 Unraveling Sleep EEG-ECG Interactions in Major Depression: Preliminary Results of a Coherence Analysis. 47, A412. doi: 10.1093/sleep/zsae067.0960.

Brandenberger, G., Ehrhart, J., Piquard, F. & Simon, C. Inverse coupling between ultradian oscillations in delta wave activity and heart rate variability during sleep. 112(6), 992–996. doi: 10.1016/S1388-2457(01)00507-7.

Catrambone, V. & Valenza, G. Nervous-System-Wise Functional Estimation of Directed Brain–Heart Interplay Through Microstate Occurrences. 70(8), 2270–2278. doi: 10.1109/TBME.2023.3240593.

Clifford, G. & Tarassenko, L. Quantifying errors in spectral estimates of HRV due to beat replacement and resampling. 52(4), 630–638. doi: 10.1109/TBME.2005.844028.

Cohen, M. X. Assessing transient cross-frequency coupling in EEG data. 168(2), 494–499. doi: 10.1016/j.jneumeth.2007.10.012.

Coppieters't Wallant, D., Muto, V., Gaggioni, G., Jaspar, M., Chellappa, S. L., Meyer, C., Vandewalle, G., Maquet, P. & Phillips, C. (2016). Automatic artifacts and arousals detection in whole-night sleep EEG recordings. *Journal of neuroscience methods*, 258, 124–133.

de Aguiar Neto, F. S. & Rosa, J. L. G. Depression biomarkers using non-invasive EEG: A review. 105, 83–93. doi: 10.1016/j.neubiorev.2019.07.021.

Ehrhart, J., Toussaint, M., Simon, C., Gronfier, C., Luthringer, R. & Brandenberger, G. Alpha activity and cardiac correlates: three types of relationships during nocturnal sleep. 111(5), 940–946. doi: 10.1016/S1388-2457(00)00247-9.

Geng, D., An, Q., Fu, Z., Wang, C. & An, H. Identification of major depression patients using machine learning models based on heart rate variability during sleep stages for pre-hospital screening. 162, 107060. doi: 10.1016/j.compbiomed.2023.107060.

Gimenez-Nadal, J. I., Lafuente, M., Molina, J. A. & Velilla, J. Resampling and bootstrap algorithms to assess the relevance of variables: applications to cross section entrepreneurship data. 56(1), 233–267. doi: 10.1007/s00181-017-1355-x.

Goldschmied, J. R., Cheng, P., Armitage, R. & Deldin, P. J. A preliminary investigation of the role of slow-wave activity in modulating waking EEG theta as a marker of sleep propensity in major depressive *disorder*. 257, 504–509. doi: 10.1016/j.jad.2019.07.027.

Goodfellow, I., Bengio, Y. & Courville, A. (2016). Deep Learning.

Hosseinifard, B., Moradi, M. H. & Rostami, R. Classifying depression patients and normal subjects using machine learning techniques and nonlinear features from EEG signal. 109(3), 339–345. doi: 10.1016/j.cmpb.2012.10.008.

INVENTORY-II, B. D. (2010). Beck depression inventory-II. *The Corsini Encyclopedia of Psychology, Volume 1*, 1, 210.

Jirsa, V. & Müller, V. (2013). Cross-frequency coupling in real and virtual brain networks. *Frontiers in computational neuroscience*, 7, 78.

Jurysta, F., Kempenaers, C., Lancini, J., Lanquart, J.-P., Van De Borne, P. & Linkowski, P. Altered interaction between cardiac vagal influence and delta sleep EEG suggests an altered neuroplasticity in patients suffering from major depressive disorder. 121(3), 236–239. doi: 10.1111/j.1600-0447.2009.01475.x.

Jurysta, F., Lanquart, J.-P., van de Borne, P., Migeotte, P.-F., Dumont, M., Degaute, J.-P. & Linkowski, P. The link between cardiac autonomic activity and sleep delta power is altered in men with sleep apnea-hypopnea syndrome. 291(4), R1165–R1171. doi: 10.1152/ajpregu.00787.2005.

Jurysta, F., van de Borne, P., Migeotte, P. F., Dumont, M., Lanquart, J. P., Degaute, J. P. & Linkowski, P. A study of the dynamic interactions between sleep EEG and heart rate variability in healthy young men. 114(11), 2146–2155. doi: 10.1016/S1388-2457(03)00215-3.

Khandoker, A., Karmakar, C. & Palaniswami, M. Interaction between sleep EEG and ECG signals during and after obstructive sleep apnea events with or without arousals. *2008 Computers in Cardiology*, pp. 685–688. doi: 10.1109/CIC.2008.4749134.

Khandoker, A. H., Karmakar, C. K. & Palaniswami, M. Analysis of coherence between sleep EEG and ECG signals during and after obstructive sleep apnea events. *2008 30th Annual International Conference of the IEEE Engineering in Medicine and Biology Society*, pp. 3876–3879. doi: 10.1109/IEMBS.2008.4650056.

Koch, C., Wilhelm, M., Salzmann, S., Rief, W. & Euteneuer, F. A meta-analysis of heart rate variability in major depression. 49(12), 1948–1957. doi: 10.1017/S0033291719001351.

Koochaki, F. & Najafizadeh, L. A Siamese Convolutional Neural Network for Identifying Mild Traumatic Brain Injury and Predicting Recovery. 32, 1779–1786. doi: 10.1109/TNSRE.2024.3391067.

Lanthier, M., Foti, M.-C., Higginson, C., Tavakoli, P., Oksit, D., Ray, L., Fogel, S. & Robillard, R. 1119 Validation of a Portable Sleep Electroencephalography Device in Good Sleepers and People with Sleep Apnea. 47, A480. doi: 10.1093/sleep/zsae067.01119.

Lecun, Y., Bottou, L., Bengio, Y. & Haffner, P. Gradient-based learning applied to document recognition. 86(11), 2278–2324. doi: 10.1109/5.726791.

Licht, C. M. M., de Geus, E. J. C., Zitman, F. G., Hoogendijk, W. J. G., van Dyck, R. & Penninx, B. W. J. H. Association Between Major Depressive Disorder and Heart Rate Variability in the Netherlands Study of Depression and Anxiety (NESDA). 65(12), 1358–1367. doi: 10.1001/archpsyc.65.12.1358.

Lázaro, J., Reljin, N., Bailón, R., Gil, E., Noh, Y., Laguna, P. & Chon, K. H. Electrocardiogram Derived Respiratory Rate Using a Wearable Armband. 68(3), 1056–1065. doi: 10.1109/TBME.2020.3004730.

Malik, M. & Camm, A. J. Heart rate variability. 13(8), 570–576. doi: 10.1002/clc.4960130811.

Moussa, M., Alzaabi, Y. & Khandoker, A. Depression in Obstructive Sleep Apnea Patients: Is Using Complex Deep Learning Structures Worth It?:. *Proceedings of the 16th International Joint Conference on Biomedical Engineering Systems and Technologies*, pp. 203–211. doi: 10.5220/0011655600003414.

Mumtaz, W. & Qayyum, A. A deep learning framework for automatic diagnosis of unipolar depression. 132, 103983. doi: 10.1016/j.ijmedinf.2019.103983.

Organization, W. H. Depression and Other Common Mental Disorders.

Pan, J. & Tompkins, W. J. A Real-Time QRS Detection Algorithm. BME-32(3), 230–236. doi: 10.1109/TBME.1985.325532.

Pinto, S. J. & Parente, M. Comprehensive review of depression detection techniques based on machine learning approach. doi: 10.1007/s00500-024-09862-1.

Rangayyan, R. M. & Krishnan, S. (2024). *Biomedical signal analysis*. John Wiley & Sons.

Rowe, K., Moreno, R., Lau, T. R., Wallooppillai, U., Nearing, B. D., Kocsis, B., Quattrochi, J., Hobson, J. A. & Verrier, R. L. Heart rate surges during REM sleep are associated with theta rhythm and PGO activity in cats. 277(3), R843–R849. doi: 10.1152/ajpregu.1999.277.3.R843.

Saad, M., Ray, L. B., Bradley-Garcia, M., Palamarchuk, I. S., Gholamrezaei, A., Douglass, A., Lee, E. K., Soucy, L. & Robillard, R. Autonomic Modulation of Cardiac Activity Across Levels of Sleep Depth in Individuals With Depression and Sleep Complaints. 82(2), 172. doi: 10.1097/PSY.0000000000000766.

Saad, M., Ray, L. B., Bujaki, B., Parvaresh, A., Palamarchuk, I., De Koninck, J., Douglass, A., Lee, E. K., Soucy, L. J., Fogel, S., Morin, C. M., Bastien, C., Merali, Z. & Robillard, R. Using heart rate profiles during sleep as a biomarker of depression. 19(1), 168. doi: 10.1186/s12888-019-2152-1.

Thayer, J. F. & Lane, R. D. A model of neurovisceral integration in emotion regulation and dysregulation. 61(3), 201–216. doi: 10.1016/S0165-0327(00)00338-4.

Tobaldini, E., Nobili, L., Strada, S., Casali, K. R., Braghiroli, A. & Montano, N. Heart rate variability in normal and pathological sleep. 4. doi: 10.3389/fphys.2013.00294.

Tsuno, N., Besset, A., Ritchie, K. et al. (2005). Sleep and depression. *Journal of clinical psychiatry*, 66(10), 1254–1269.

Wang, Y., Sokhadze, E. M., El-Baz, A. S., Li, X., Sears, L., Casanova, M. F. & Tasman, A. Relative Power of Specific EEG Bands and Their Ratios during Neurofeedback Training in Children with Autism Spectrum Disorder. 9, 723. doi: 10.3389/fnhum.2015.00723.

Zhang, B., Zhou, W., Cai, H., Su, Y., Wang, J., Zhang, Z. & Lei, T. Ubiquitous Depression Detection of Sleep Physiological Data by Using Combination Learning and Functional Networks. 8, 94220–94235. doi: 10.1109/ACCESS.2020.2994985.

Zhang, Y., Wang, K., Wei, Y., Guo, X., Wen, J. & Luo, Y. Minimal EEG channel selection for depression detection with connectivity features during sleep. 147, 105690. doi: 10.1016/j.compbiomed.2022.105690.